

Supporting Information for:

Synthesis and Reduction Chemistry of Mixed-Lewis-Base-Stabilised Chloroborylenes

Merle Arrowsmith,^a Julia I. Schweizer,^b Myron Heinz,^b Marcel Härtelich,^a Ivo Krummenacher,^a Max C. Holthausen,^b Holger Braunschweig*,^a

^a Institut für Anorganische Chemie and the Institute for Sustainable Chemistry & Catalysis with Boron, Julius-Maximilians-Universität Würzburg, Am Hubland, 97074 Würzburg, Germany.

^b Institut für Anorganische und Analytische Chemie, Goethe-Universität Frankfurt am Main, Max-von-Laue-Str. 7, 60438 Frankfurt am Main, Germany.

Table of contents

<u>Methods and materials</u>	2
<u>NMR spectra of isolated compounds</u>	9
<u>EPR spectrum of radical 2</u>	27
<u>UV-vis spectra of compounds 2 and 3-L</u>	28
<u>Cyclic voltammetry</u>	29
<u>X-ray crystallographic data</u>	33
<u>Computational details</u>	37
<u>References</u>	43

Methods and materials

All manipulations were performed either under an atmosphere of dry argon or *in vacuo* using standard Schlenk line or glovebox techniques. Deuterated solvents were dried over molecular sieves and degassed by three freeze-pump-thaw cycles prior to use. All other solvents were distilled and degassed from appropriate drying agents. Solvents (both deuterated and non-deuterated) were stored under argon over activated 4 Å molecular sieves. NMR spectra were acquired on a Bruker Avance 500 NMR spectrometer (^1H and $^1\text{H}\{^{11}\text{B}\}$: 500.1 MHz, $^{11}\text{B}\{^1\text{H}\}$: 160.5 MHz, $^{13}\text{C}\{^1\text{H}\}$ and $^{13}\text{C}\{^1\text{H},^{11}\text{B}\}$: 125.8 MHz). Chemical shifts (δ) are given in ppm and internally referenced to the carbon nuclei ($^{13}\text{C}\{^1\text{H}\}$) or residual protons (^1H) of the solvent. $^{11}\text{B}\{^1\text{H}\}$ NMR spectra were referenced to $[\text{BF}_3 \cdot \text{OEt}_2]$ as an external standard. UV/Vis spectra were acquired on a JASCO-V660 UV/Vis spectrometer under inert conditions inside a glovebox. Cyclic voltammetry experiments were performed using a Gamry Instruments Reference 600 potentiostat. Microanalyses (C, H, N) were performed on an Elementar vario MICRO cube elemental analyzer. High-resolution mass spectrometry data were obtained from a Thermo Scientific Exactive Plus spectrometer in ASAP or LIFDI mode.

Note: Microanalyses (C, H, N) were only performed of $(\text{CAAC}^{\text{Me}})_2\text{BCl}$ and $(\text{CAAC}^{\text{Me}})(\text{IMes})\text{BCl}$. The data shown herein required multiple attempts and provided the best fit for the calculated analysis. On average carbon content was off by 0.4 – 0.8%, hydrogen content by 0.2 – 0.7% and nitrogen by less than 0.4% despite tight wrapping of samples in three layers of aluminium foil and less than 5 min between removal from the glovebox in a sealed vial and the measurement. Given these results, which show how extremely air- and moisture-sensitive the compounds are, all other borylenes were analyzed by liquid injection field desorption ionisation mass spectrometry (LIFDI-MS) under inert atmosphere instead.

Solvents and reagents were purchased from Sigma Aldrich or Alfa Aesar. CAAC^{Me} (1-(2,6-diisopropylphenyl)-3,3,5,5-tetramethylpyrrolidin-2-ylidene),¹ IMes (1,3-bis(2,4,6-trimethylphenyl)imidazol-2-ylidene),² SIMes (1,3-bis(2,4,6-trimethylphenyl)-4,5-dihydroimidazol-2-ylidene),³ IMe^{Me} (1,3,4,5-tetramethylimidazol-2-ylidene)⁴ and KC_8 ⁵ were synthesised using literature procedures.

(CAAC^{Me})BCl₃, 1

500 mg CAAC^{Me} (1.70 mmol) and 314 mg of BCl₃·SMe₂ (1.70 mmol) were combined in 5 mL benzene at room temperature. The reaction was very exothermic and a colourless precipitate rapidly formed. The reaction mixture was left undisturbed for 18 h at room temperature prior to filtration and drying of the colourless product, adduct **1**, *in vacuo* (670 mg, 1.66 mmol, 98% yield). ¹H NMR (400 MHz, C₆D₆, 297 K): δ = 7.09 (t, 1H, ³J = 7.9 Hz, *p*-Dip-H), 6.97 (d, 2H, ³J = 7.9 Hz, *m*-Dip-H), 2.67 (sept, 2H, ³J = 6.6 Hz, *i*Pr-CH), 1.77 (s, 6H, NC(CH₃)₂), 1.52 (d, 6H, ³J = 6.6 Hz, *i*Pr-CH₃), 1.43 (s, 2H, CH₂), 1.07 (d, 6H, ³J = 6.6 Hz, *i*Pr-CH₃), 0.80 (s, 6H, C(CH₃)₂) ppm. ¹³C{¹H} NMR (101 MHz, C₆D₆, 297 K): δ = 213.4 (br.; C_{carbene}, detected by HMBC), 145.9 (*o*-C_{Dip}), 133.2 (*i*-C_{Dip}), 130.6 (*p*-C_{Dip}), 125.7 (*m*-C_{Dip}), 80.0 (NCMe₂), 54.9 (CMe₂), 51.6 (CH₂), 31.2 (C(CH₃)₂), 29.9 (NC(CH₃)₂), 28.7 (*i*Pr-CH), 26.8 (*i*Pr-CH₃), 24.9 (*i*Pr-CH₃) ppm. ¹¹B NMR (128 MHz, C₆D₆, 297 K): δ = 3.2 ppm. Elemental analysis for C₂₀H₃₁BCl₃N (M_w = 402.6) calcd: C 59.66, H 7.76 N 3.48%; found: C 59.42, H 7.88, N 3.46%.

[(CAAC^{Me})BCl₂]⁺, 2

200 mg **1** (0.50 mmol) and 3.5 mg lithium sand (0.50 mmol) were combined in 0.5 mL THF at room temperature and the mixture was vigorously stirred until the complete disappearance of any metallic lithium, at which point the solution had become pale green. After removal of the solvent and extraction with 0.5 mL hexane the filtrate was stored overnight at -25 °C, yielding a small crop of orange crystals of **2** (48 mg, 0.13 mmol, 26% yield). Although EPR spectroscopic analysis of the mother liquor showed that it still contained large amounts of **2**, further crystallisation proved difficult due to its very high solubility even in minimal amounts of pentane at low temperature. Elemental analysis for C₂₀H₃₁BCl₂N (M_w = 367.2) calcd: C 65.42, H 8.51, N 3.81%; found: C 65.35, H 8.92, N 3.57%.

General procedure for the synthesis of 3-L (L = CAAC^{Me}, IMes, SIMes)

1 (1 equiv.), L (1 equiv.) and KC₈ (2.5 equiv.) were combined in benzene at room temperature and the reaction mixture stirred for two hours at room temperature. After removal of all volatiles *in vacuo* the solid residue was extracted with 3 x 1 mL hexane. The filtrate was reduced *in vacuo* to 0.5 mL and stored in the freezer at –25 °C to provide crystals of the desired borylenes.

(CAAC^{Me})₂BCl, 3-CAAC^{Me}

15.7 mg **1** (39 µmol), 11.1 mg CAAC^{Me} (39 µmol) and 13.2 mg KC₈ (97 µmol). Recrystallisation from 0.2 mL pentane at –25 °C over a period of one week yielded deep purple crystals of **3-CAAC^{Me}** (15 mg, 24 µmol, 62%). *Note: the reaction could not be cleanly scaled up due to increasing amounts of overreduction to (CAAC^{Me})₂BH (**4**) at larger scales.* ¹H NMR (400 MHz, C₆D₆, 297 K): 7.12 (t, 1H, ³J = 7.5 Hz, *p*-Dip-H), 7.11 (br. d, 2H, ³J = 7.5 Hz, *m*-Dip-H), 3.19 (sept, 2H, ³J = 6.8 Hz, *i*Pr-CH), 1.85 (s, 6H, NC(CH₃)₂), 1.81 (s, 2H, CH₂), 1.31 (br. d, 6H, ³J = 6.8 Hz, *i*Pr-CH₃), 1.25 (d, 6H, ³J = 6.8 Hz, *i*Pr-CH₃), 1.08 (s, 6H, C(CH₃)₂) ppm. ¹³C{¹H} NMR (101 MHz, C₆D₆, 297 K): δ = 147.4 (*i*-C_{Dip}), 141.1 (*o*-C_{Dip}), 127.2 (*p*-C_{Dip}), 124.5 (*m*-C_{Dip}), 69.0 (NCMe₂), 60.2 (CH₂), 47.3 (CMe₂), 34.8 (C(CH₃)₂), 30.4 (NC(CH₃)₂), 29.4 (*i*Pr-CH), 26.4 (*i*Pr-CH₃), 25.7 (*i*Pr-CH₃) ppm. *Note: the BC_{CAAC} resonance could not be detected by HMBC.* ¹¹B NMR (128 MHz, C₆D₆, 297 K): δ = 18.7 (br.) ppm. Elemental analysis for C₄₀H₆₂BClN₂ (*M*_w = 616.5) calcd: C 77.84, H 10.13, N 4.54%; found: C 77.38, H 10.29, N 4.65%. LIFDI-MS for [C₄₀H₆₂BClN₂ + H]⁺ calcd: 617.4767; found: 617.4755.

(CAAC^{Me})(IMes)BCl, 3-IMes

70 mg **1** (0.17 mmol), 53 mg IMes (0.17 mmol) and 59 mg KC₈ (0.43 mmol). Analytically pure **3-IMes** was isolated as purple-pink crystals (63 mg, 99 µmol, 58% yield). ¹H NMR (500 MHz, C₆D₆, 297 K): δ = 7.17-7.20 (m, 1H, *p*-Dip-H), 7.11 (br. d, 2H, ³J = 7.3 Hz, *m*-Dip-H), 6.77, 6.72 (two s, 2H each, *m*-Mes-H), 5.92 (s, 2H, NCH), 3.49 (sept, 2H, ³J = 6.8 Hz, *i*Pr-CH), 2.25, 2.15 (two s, 6H each, *o*-Mes-CH₃), 2.11 (s, 6H, *p*-Mes-CH₃), 1.92 (s, 2H, CH₂), 1.36, 1.25 (two d, 6H each, ³J = 6.8 Hz, *i*Pr-CH₃), 1.22 (s, 6H, NC(CH₃)₂), 1.13 (s, 6H, C(CH₃)₂) ppm. ¹³C{¹H} NMR (126 MHz, C₆D₆, 297 K): δ = 166.1 (BC_{IMes}, identified by HMBC), 154.1 (BC_{CAAC}, identified by HMBC), 151.0 (*i*-C_{Dip}), 141.9 (*o*-C_{Dip}), 138.8 (*p*-C_{Mes}), 137.3 (*o*-C_{Mes}), 136.8 (*i*-C_{Mes}), 134.6 (*o*-C_{Mes}), 130.4 (*m*-C_{Mes}), 130.3 (*m*-C_{Mes}), 126.5 (*p*-C_{Dip}), 123.6 (*m*-C_{Dip}), 122.1 (NCH), 64.4 (NCMe₂), 60.6 (CH₂), 43.4 (CMe₂), 33.1 (C(CH₃)₂), 30.9 (NC(CH₃)₂), 29.0 (*i*Pr-CH), 26.5 (*i*Pr-CH₃), 25.9 (*i*Pr-CH₃), 21.3 (*p*-Mes-CH₃), 20.2 (*o*-Mes-CH₃), 19.9 (*o*-Mes-CH₃)

ppm. ^{11}B NMR (160 MHz, C_6D_6 , 297 K): $\delta = 8.4$ (br.) ppm. Elemental analysis for $\text{C}_{41}\text{H}_{55}\text{BClN}_3$ ($M_w = 635.4$) calcd: C 77.41, H 8.71, N 6.61%; found: C 78.15, H 9.35, N 6.65%. LIFDI-MS for $[\text{C}_{41}\text{H}_{55}\text{BClN}_3 + \text{H}]^+$ calcd: 636.4250; found: 636.4268.

(CAAC^{Me})(SIMes)BCl, 3-SIMes

200 mg **1** (0.50 mmol), 155 mg SIMes (0.50 mmol) and 168 mg KC_8 (1.24 mmol). Analytically pure **3-SIMes** was isolated as dark pink crystals (242 mg, 0.38 mmol, 76% yield). ^1H NMR (500 MHz, C_6D_6 , 297 K): $\delta = 7.14$ (t, 1H, $^3J = 7.7$ Hz, *p*-Dip-H), 7.03 (d, 2H, $^3J = 7.7$ Hz, *m*-Dip-H), 6.79, 6.74 (two s, 2H each, *m*-Mes-H), 3.19 (sept, 2H, $^3J = 6.8$ Hz, *iPr*-CH), 3.01-3.12 (AB system of two m, 4H, NCH_2), 2.39, 2.35 (two s, 6H each, *o*-Mes-CH₃), 2.14 (s, 6H, *p*-Mes-CH₃), 1.87 (s, 2H, CH₂), 1.39 (s, 6H, NC(CH₃)₂), 1.27, 1.21 (two d, 6H each, $^3J = 6.8$ Hz, *iPr*-CH₃), 1.11 (s, 6H, C(CH₃)₂) ppm. $^{13}\text{C}\{\text{H}\}$ NMR (126 MHz, C_6D_6 , 297 K): $\delta = 167.6$ (BC_{CAAC}, identified by HMBC), 149.6 (*i*-C_{Dip}), 141.8 (*o*-C_{Dip}), 140.6 (*p*-C_{Mes}), 136.7 (*o*-C_{Mes}), 136.1 (*i*-C_{Mes}), 134.5 (*o*-C_{Mes}), 130.8 (*m*-C_{Mes}), 130.2 (*m*-C_{Mes}), 127.7 (*p*-C_{Dip}), 123.7 (*m*-C_{Dip}), 66.6 (NCMe₂), 59.5 (CH₂), 52.7 (NCH₂), 45.2 (CMe₂), 32.0 (C(CH₃)₂), 30.7 (NC(CH₃)₂), 29.2 (*iPr*-CH), 26.2 (*iPr*-CH₃), 25.6 (*iPr*-CH₃), 21.2 (*p*-Mes-CH₃), 20.9 (*o*-Mes-CH₃), 20.7 (*o*-Mes-CH₃) ppm. Note: the BC_{SIMes} resonance could not be detected. ^{11}B NMR (160 MHz, C_6D_6 , 297 K): $\delta = 11.9$ (br.) ppm. LIFDI-MS for $[\text{C}_{41}\text{H}_{57}\text{BClN}_3]$ calcd: 637.4329; found: 637.4321.

General procedure for the synthesis of 3-PR₃ (L = PEt₃, PMe₃)

PR₃ (5 equiv.) and KC_8 (2.5 equiv.) were combined in benzene at room temperature. A dilute benzene solution of **1** (1 equiv.) was added dropwise to this mixture under vigorous stirring. The resulting reaction mixture was stirred for two hours at room temperature, after which all volatiles were removed *in vacuo* and the solid residue extracted with 3 x 1 mL of a 1:1 hexane/toluene mixture. The filtrate was reduced *in vacuo* to 0.5 mL and stored in the freezer at -25 °C to provide crystals of the desired borylenes.

(CAAC^{Me})(PEt₃)BCl, 3-PEt₃

200 mg **1** (0.50 mmol), 0.40 mL PEt₃ (2.70 mmol) and 168 mg KC_8 (1.24 mmol). Analytically pure **3-PEt₃** was isolated as pale yellow crystals (108 mg, 0.24 mmol, 48% yield). ^1H NMR (500 MHz, C_6D_6 , 297 K): $\delta = 7.27$ (dd, 1H, $^3J = 6.7, 8.4$ Hz, *p*-Dip-H), 7.20 (two overlapping d, 2H, $^3J = 6.3, 8.7$ Hz, *m*-Dip-H), 3.71 (sept, 2H, $^3J = 6.8$ Hz, *iPr*-CH), 2.00 (s, 2H, CH₂), 1.61 (d, 6H, $^3J = 6.8$ Hz, *iPr*-CH₃), 1.50 (s, 6H, NC(CH₃)₂), 1.39-1.45 (overlapping dq + d, 6H each, $^1J_{\text{H}-31\text{P}} = 9.9$ Hz, $^3J_{\text{H}-1\text{H}} = 7.6$ Hz, P(CH₂CH₃)₃, $^3J_{\text{H}-1\text{H}} = 6.8$ Hz, *iPr*-CH₃), 1.33 (s, 6H,

$\text{C}(\text{CH}_3)_2$), 0.73 (dt, 9H, $^4J_{\text{IH}-\text{31P}} = 16.1$ Hz, $^3J_{\text{IH}-\text{IH}} = 7.6$ Hz, P($\text{CH}_2\text{CH}_3)_3$) ppm. $^{13}\text{C}\{\text{H}\}$ NMR (126 MHz, C_6D_6 , 297 K): $\delta = 164.7$ (BC_{CAAC} , identified by HMBC), 150.3 (*i*-C_{Dip}), 142.5 (*o*-C_{Dip}), 126.8 (*p*-C_{Dip}), 124.1 (*m*-C_{Dip}), 64.6 (NCMe₂), 61.3 (CH_2), 43.7 (CMe₂), 36.3 (C(CH₃)₂), 29.9 (NC(CH₃)₂), 29.0 (*iPr*-CH), 26.0 (*iPr*-CH₃), 25.7 (*iPr*-CH₃), 15.1 (d, $^1J_{\text{13C-31P}} = 43.8$ Hz, P($\text{CH}_2\text{CH}_3)_3$), 7.35 (d, $^2J_{\text{13C-31P}} = 3.2$ Hz, P($\text{CH}_2\text{CH}_3)_3$) ppm. ^{11}B NMR (160 MHz, C_6D_6 , 297 K): $\delta = 2.8$ (d, $^1J_{\text{11B-31P}} = 175$ Hz) ppm. ^{31}P NMR (202 MHz, C_6D_6 , 297 K): $\delta = 4.19$ (m, fwmh ≈ 550 Hz) ppm. LIFDI-MS for [C₂₆H₄₆BCINP] calcd: 449.3144; found: 449.3135.

(CAAC^{Me})(PMe₃)BCl, 3-PMe₃

500 mg **1** (1.2 mmol), 0.50 mL PMe₃ (4.8 mmol) and 420 mg KC₈ (3.1 mmol). Analytically pure **3-PMe₃** was isolated as pale yellow crystals (240 mg, 0.59 mmol, 49% yield). ^1H NMR (500 MHz, C_6D_6 , 297 K): $\delta = 7.25$ (dd, 1H, $^3J = 6.3, 8.7$ Hz, *p*-Dip-H), 7.19 (two overlapping d, 2H, $^3J = 6.3, 8.7$ Hz, *m*-Dip-H), 3.69 (sept, 2H, $^3J = 6.8$ Hz, *iPr*-CH), 1.97 (s, 2H, CH₂), 1.55 (d, 6H, $^3J = 6.8$ Hz, *iPr*-CH₃), 1.48 (s, 6H, NC(CH₃)₂), 1.39 (d, 6H, $^3J = 6.8$ Hz, *iPr*-CH₃), 1.34 (s, 6H, C(CH₃)₂), 0.90 (s, $^2J_{\text{IH-31P}} = 11.0$ Hz, 9H, PCH₃) ppm. $^{13}\text{C}\{\text{H}\}$ NMR (126 MHz, C_6D_6 , 297 K): $\delta = 161.7$ (BC_{CAAC} , identified by HMBC), 149.8 (*i*-C_{Dip}), 142.9 (*o*-C_{Dip}), 126.6 (*p*-C_{Dip}), 124.2 (*m*-C_{Dip}), 64.5 (NCMe₂), 61.3 (CH₂), 43.8 (CMe₂), 35.9 (C(CH₃)₂), 29.9 (NC(CH₃)₂), 28.8 (*iPr*-CH), 25.9 (*iPr*-CH₃), 25.5 (*iPr*-CH₃), 15.1 (d, $^1J_{\text{13C-31P}} = 47.7$ Hz, PCH₃) ppm. ^{11}B NMR (160 MHz, C_6D_6 , 297 K): $\delta = 5.6$ (d, $^1J_{\text{11B-31P}} = 169$ Hz) ppm. ^{31}P NMR (202 MHz, C_6D_6 , 297 K): $\delta = -24.7$ (m, fwmh ≈ 570 Hz) ppm. LIFDI-MS for [C₂₃H₄₀BCINP + H]⁺ calcd: 408.2753; found: 408.2747; for [C₂₃H₄₀BCINP – PMe₃] calcd: 332.2311; found: 332.2303.

(CAAC^{Me})(IMe^{Me})BCl, 3-IMe^{Me}

One equiv. IMe^{Me} (7.6 mg, 61 μmol) was added to a 5:1 hexane/benzene solution of **3-PMe₃** (25 mg, 61 μmol). The solution slowly turned deep red over a period of 2 h at room temperature and a red precipitate formed, which was collected and dried in vacuo, yielding 15.2 mg of analytically pure **3-IMe^{Me}** (33 μmol , 55% yield). Red single crystals suitable for X-ray crystallographic analysis were obtained by slow evaporation of the solvent under an inert atmosphere. ^1H NMR (500 MHz, C_6D_6 , 297 K): $\delta = 7.33\text{--}7.40$ (m, 3H, Dip-H), 4.02 (sept, 2H, $^3J = 6.8$ Hz, *iPr*-CH), 3.27 (s, 6H, NCH_{3-IMeMe}), 2.08 (s, 2H, CH₂), 1.80, 1.58 (two d, 6H each, $^3J = 6.8$ Hz, *iPr*-CH₃), 1.46 (s, 6H, NC(CH₃)₂), 1.23 (s, 6H, C(CH₃)₂), 1.19 (s, 6H, CCH_{3-IMeMe}) ppm. $^{13}\text{C}\{\text{H}\}$ NMR (126 MHz, C_6D_6 , 297 K): $\delta = 163.7$ (BC_{IMeMe} , identified by HMBC), 151.8 (*o*-C_{Dip}), 147.1 (BC_{CAAC} , identified by HMBC), 141.9 (*i*-C_{Dip}), 126.6 (*p*-C_{Dip}), 124.1 (*m*-C_{Dip}), 123.8 (NCMe-_{IMeMe}), 63.2 (NCMe₂), 60.2 (CH₂), 43.3 (CMe₂), 34.2 (C(CH₃)₂), 33.9 (NCH₃).

{IMeMe}) 30.4 (NC(CH₃)₂), 29.0 (*i*Pr-CH), 26.4 (*i*Pr-CH₃), 26.0 (*i*Pr-CH₃), 8.4 (CCH{3-IMeMe}) ppm. ¹¹B NMR (160 MHz, C₆D₆, 297 K): δ = 5.5 (br.) ppm. LIFDI-MS for [C₂₇H₄₃BClN₃ + H]⁺ calcd: 456.3311; found: 456.3325.

[CAAC^{Me}]BCl₂]K₂(SMe₂), 4

40 mg of **1** (99 μmol) was suspended in 0.4 mL of toluene and 0.1 mL of SMe₂ was added. After addition of 30 mg of KC₈ (0.22 mmol), the reaction mixture was stirred for 18 h at rt. The brown suspension was filtered and the filtrate stored at -25 °C for 3 weeks until a few red crystals of **4** could be isolated and structurally analyzed. Unfortunately, repeated attempts never yielded more than a few crystals of **4**, thus preventing full characterisation.

(CAAC^{Me})₂BH, 5-CAAC^{Me}

40 mg **3-CAAC^{Me}** (65 μmol) and 18 mg KC₈ (0.13 mmol) were combined in benzene at rt and the reaction mixture stirred for 2 h, at which point full conversion of **3-CAAC^{Me}** to two products was determined by ¹¹B NMR spectroscopy: **5-CAAC^{Me}** (ca. 40%) and a second, unidentified product (ca. 60%) presenting a very broad resonance centred at 54 ppm. Crystallisation from pentane at -25 °C provided single crystals of **5-CAAC^{Me}** suitable for X-ray diffraction analysis but repeated attempts to isolate sufficient amounts of pure **5-CAAC^{Me}** for full characterisation failed. ¹¹B NMR (128 MHz, C₆D₆, 297 K): δ = 12.6 (br. d) ppm. LIFDI-MS for [C₄₀H₆₂BN₂ + H]⁺ calcd: 582.5084; found: 582.5064.

(CAAC^{Me})(4-Li(thf)₃-IMes)BH, 6

Lithium sand (1.7 mg, 0.24 mmol) was added to a 0.5 mL of a THF solution of **3-IMes** (50 mg, 79 μmol). The reaction mixture was sonicated for 30 minutes, turning from purple to orange, at which point ¹¹B NMR spectroscopy showed complete conversion to a new species displaying a broad resonance at 3.4 ppm. After filtration and storage of the filtrate for 24 h at -25 °C, a small crop of orange crystals of compound **6** was obtained (26 mg, 32 μmol, 40% yield). *Note: compound 7 was extremely sensitive so that upon drying in vacuo isolated crystals systematically underwent a small amount of hydrolysis, which is why all NMR spectra are contaminated with (CAAC^{Me})(IMes)BH. Brief exposure of the NMR sample to air completed the hydrolysis (CAAC^{Me})(IMes)BH (vide infra).* ¹H{¹¹B} NMR (500 MHz, C₆D₆, 297 K): δ = 7.13-7.22 (m, 3H, Dip-H), 6.86, 6.67 (two s, 2H each, *m*-Mes-H), 5.98 (br. s, 1H, NCH), 3.54 (sept, 2H, ³J = 6.8 Hz, *i*Pr-CH), 3.38 (m, 12H, THF), 2.65 (br. s, BH), 2.28 (s, 6H, *o*-Mes-CH₃), 2.21, 2.14 (two s, 3H each, *p*-Mes-CH₃), 2.09 (s, 6H, *o*-Mes-CH₃), 2.03 (s, 2H, CH₂), 1.39 (d, 6H, ³J

$= 6.8$ Hz, *iPr-CH₃*), 1.32 (m, 12H, THF), 1.28 (s, 6H, NC(CH₃)₂), 1.25 (s, 6H, C(CH₃)₂), 1.18 (d, 6H, $^3J = 6.8$ Hz, *iPr-CH₃*) ppm. $^{13}\text{C}\{\text{H}\}$ NMR (126 MHz, C₆D₆, 297 K): $\delta = 152.0$ (*o*-C_{Dip}), 143.5 (*i*-C_{Mes}), 141.4 (*i*-C_{Dip}), 138.5 (*i*-C_{Mes}), 137.1 (*p*-C_{Mes}), 136.0 (*o*-C_{Mes}), 135.5 (*o*-C_{Mes}), 130.0 (*m*-C_{Mes}), 129.8 (NCH), 129.6 (*m*-C_{Mes}), 126.2 (*m*-C_{Dip}), 123.9 (*p*-C_{Dip}), 68.3 (THF), 63.2 (NCMe₂), 61.0 (CH₂), 43.2 (CMe₂), 33.2 (C(CH₃)₂), 30.4 (NC(CH₃)₂), 28.7 (*iPr-CH*), 28.0 (*iPr-CH₃*), 25.9 (THF), 25.3 (*iPr-CH₃*), 21.3 (*p*-Mes-CH₃), 21.2 (*p*-Mes-CH₃), 20.0 (*o*-Mes-CH₃), 19.7 (*o*-Mes-CH₃) ppm. Note: neither the BC_{CAAC} nor the BC_{IMes} resonance could be detected. ^{11}B NMR (160 MHz, C₆D₆, 297 K): $\delta = 2.8$ (br.) ppm.

(CAAC^{Me})(IMes)BH, 5-IMes

An NMR sample of **6** was very briefly exposed to air prior to flushing with argon, resulting in complete hydrolysis to **5-IMes**. Alternatively, **5-IMes** was obtained by the reduction of 3-IMes with 2 equiv. KC₈ in C₆D₆, albeit less selectively than via the first route. $^1\text{H}\{\text{B}\}$ NMR (500 MHz, C₆D₆, 297 K): $\delta = 7.12$ -7.16 (m, 3H, Dip-*H*), 6.71 (s, 4H, *m*-Mes-*H*), 5.85 (s, 2H, NCH), 3.31 (sept, 2H, $^3J = 6.8$ Hz, *iPr-CH*), 2.16 (broad s, BH), 2.15 (s, 6H, *p*-Mes-CH₃), 2.14 (s, 12H, *o*-Mes-CH₃), 1.91 (s, 2H, CH₂), 1.33 (d, 6H, $^3J = 6.8$ Hz, *iPr-CH₃*), 1.17 (s, 6H, NC(CH₃)₂), 1.10 (d, 6H, $^3J = 6.8$ Hz, *iPr-CH₃*), 1.03 (s, 6H, C(CH₃)₂) ppm. $^{13}\text{C}\{\text{H}\}$ NMR (126 MHz, C₆D₆, 297 K): $\delta = 174.2$ (BC_{CAAC}, detected by HMBC), 150.6 (*o*-C_{Dip}), 139.2 (*i*-C_{Dip}), 137.7 (*i*-C_{Mes}), 137.1 (*p*-C_{Mes}), 135.9 (*o*-C_{Mes}), 129.7 (*m*-C_{Mes}), 126.5 (*p*-C_{Dip}), 123.7 (*m*-C_{Dip}), 120.0 (NCH), 64.3 (NCMe₂), 59.7 (CH₂), 43.4 (CMe₂), 31.8 (C(CH₃)₂), 30.0 (NC(CH₃)₂), 28.5 (*iPr-CH*), 27.7 (*iPr-CH₃*), 24.6 (*iPr-CH₃*), 21.0 (*p*-Mes-CH₃), 18.9 (*o*-Mes-CH₃) ppm. Note: the BC_{IMes} resonance could not be detected. ^{11}B NMR (160 MHz, C₆D₆, 297 K): $\delta = 1.5$ (br. d) ppm. LIFDI-MS for [C₄₁H₅₆BN₃ + H]⁺ calcd: 602.4646; found: 602.4657.

(CAACH^{Me})B=(*o*-CH₂-SIMes), 7

Lithium sand (1.7 mg, 0.24 mmol) was added to a 0.5 mL of a THF solution of **3-SIMes** (50 mg, 79 μmol). The reaction mixture was sonicated for 3 h at which point it had turned dark red and displayed one major broad ^{11}B NMR resonance at -3.0 ppm (ca. 60%) besides three minor resonances at $\delta_{11\text{B}} = 3.0$ ($\approx 20\%$), 18.5 ($\approx 10\%$) and 31.4 ($\approx 10\%$) ppm. After filtration and removal of volatiles, the red residue was redissolved in 0.2 mL DME and the solution stored for 48 h at -25°C , yielding a small crop of dark red crystals of compound **7** suitable for X-ray diffraction analysis was obtained. Unfortunately, the amount of **7** isolated was insufficient for full NMR characterisation. ^{11}B NMR (128.3 MHz, C₆D₆, 297 K): $\delta = -3.0$ (broad) ppm. ^7Li NMR (155.5 MHz, C₆D₆, 297 K): $\delta = 1.3$ (broad) ppm.

NMR spectra of isolated compounds

Figure S1. ^1H NMR spectrum of **1** in C_6D_6 .

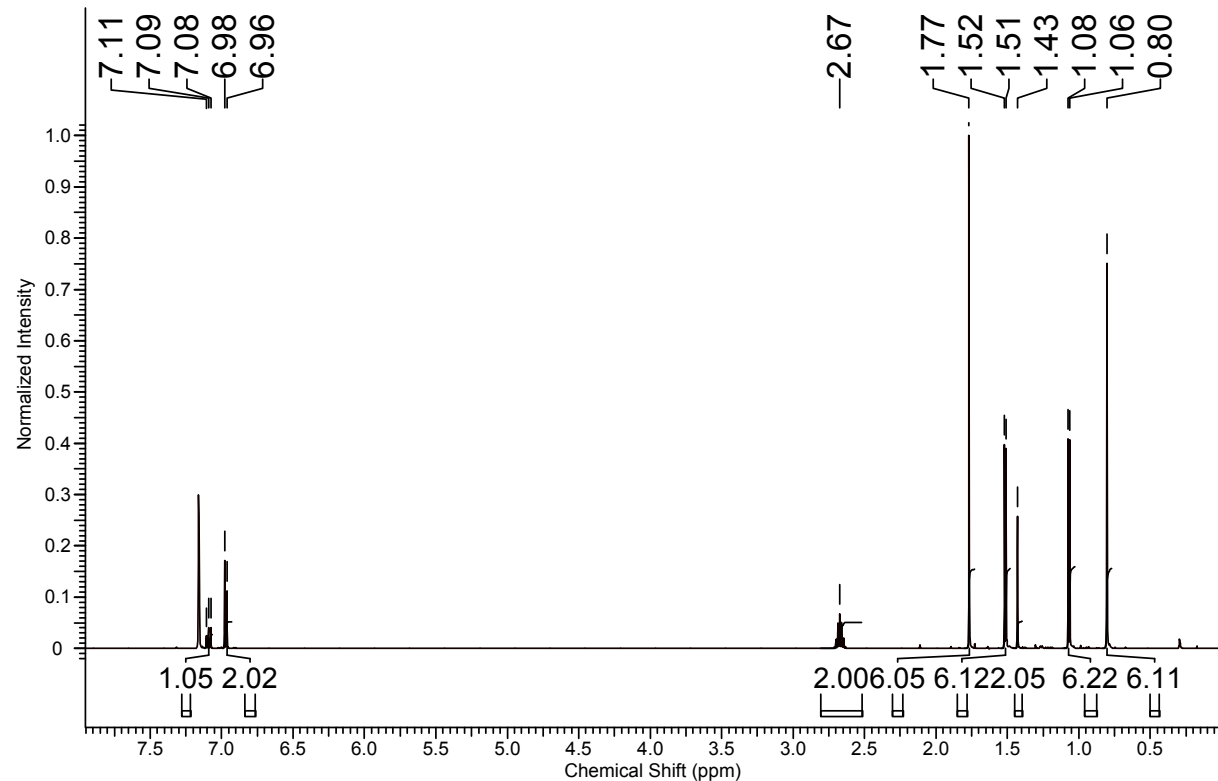


Figure S2. $^{13}\text{C}\{\text{H}\}$ NMR spectrum of **1** in C_6D_6 .

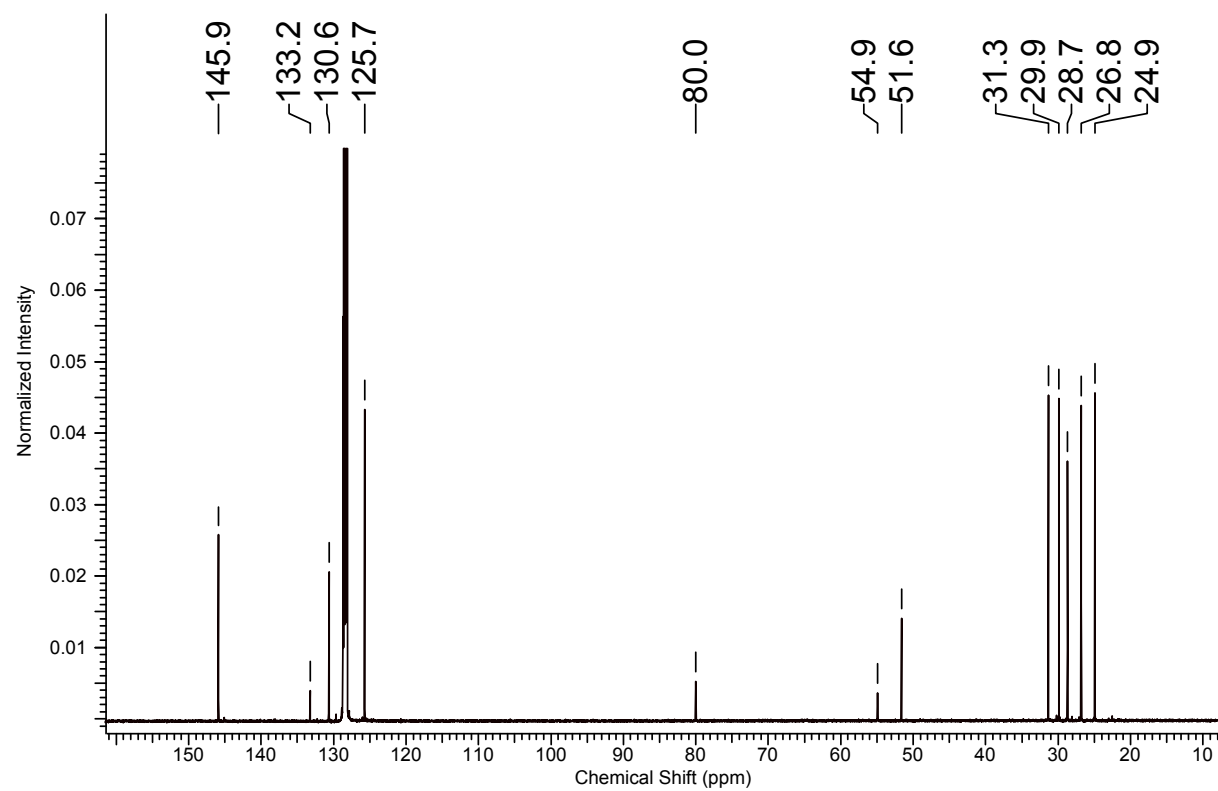


Figure S3. ^{11}B NMR spectrum of **1** in C_6D_6 . The additional resonance at 8.2 ppm is a frequently observed artefact on this NMR spectrometer.

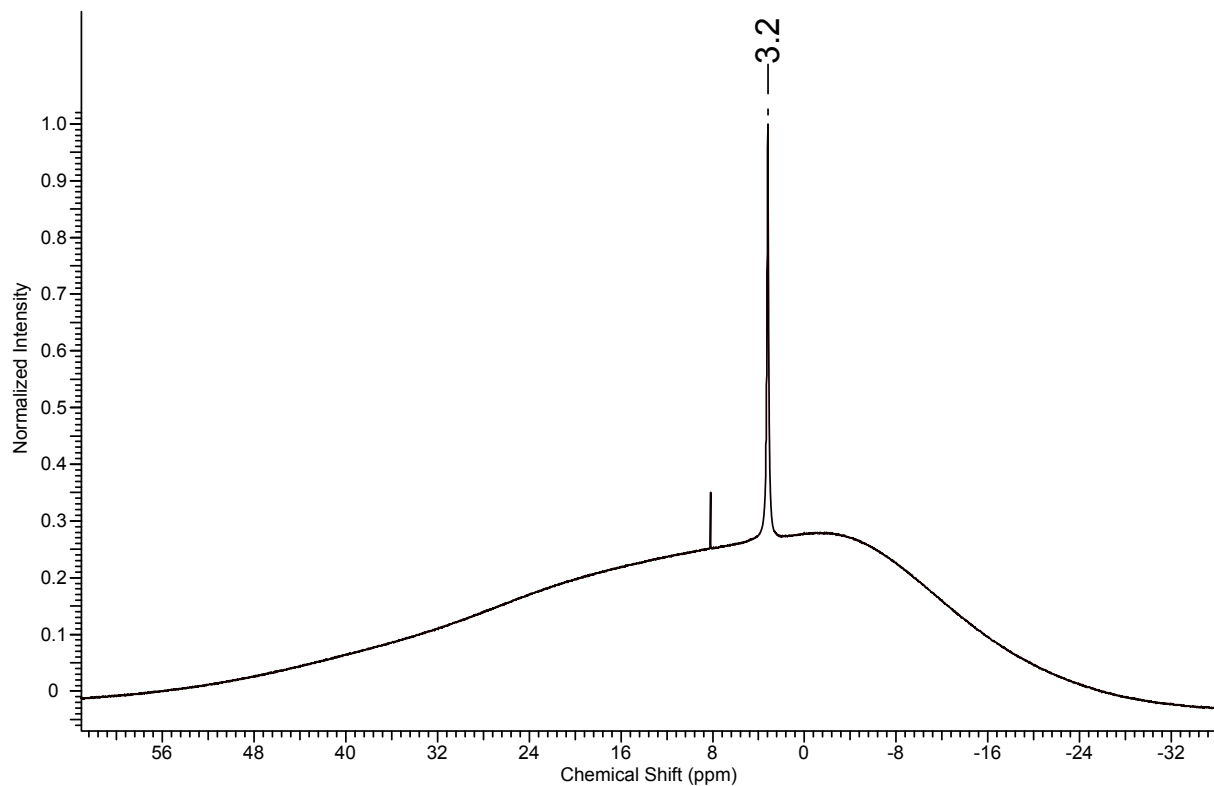


Figure S4. ^1H NMR spectrum of **3-CAAC^{Me}** in C_6D_6 .

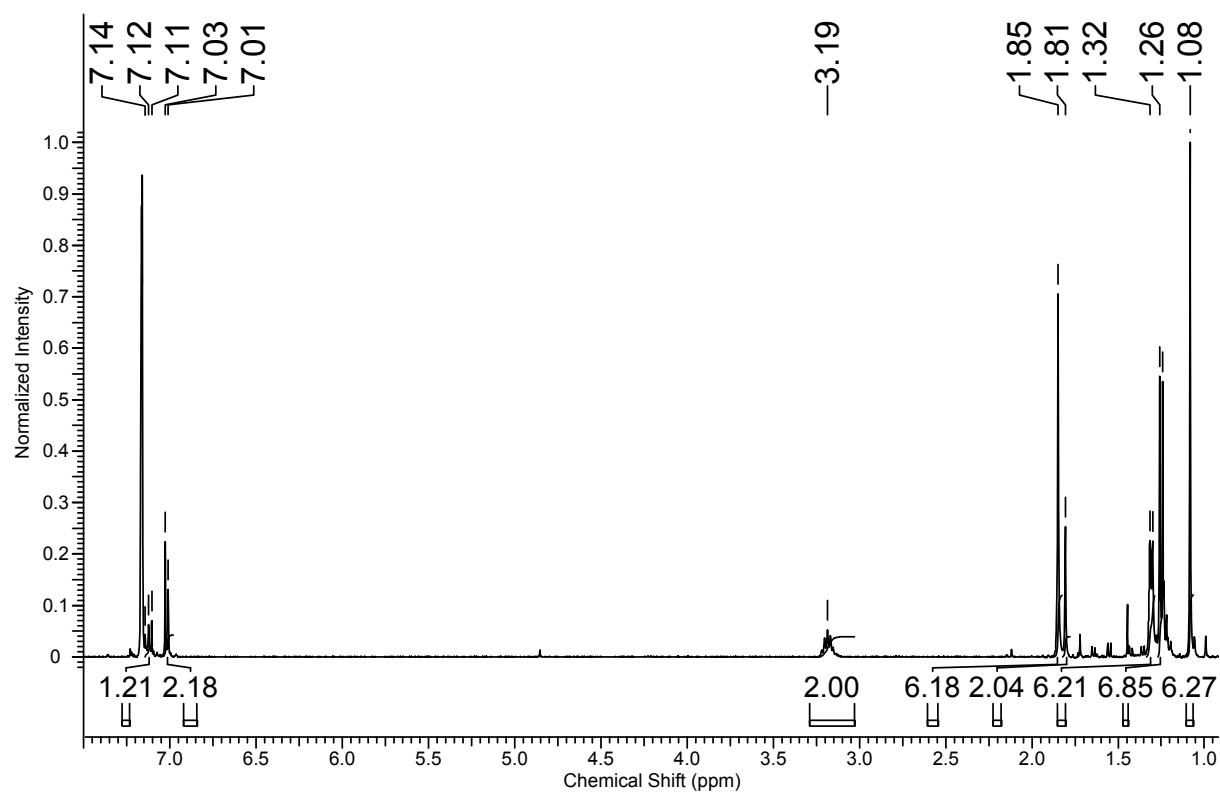


Figure S5. $^{13}\text{C}\{^1\text{H}\}$ NMR spectrum of **3-CAAC^{Me}** in C_6D_6 .

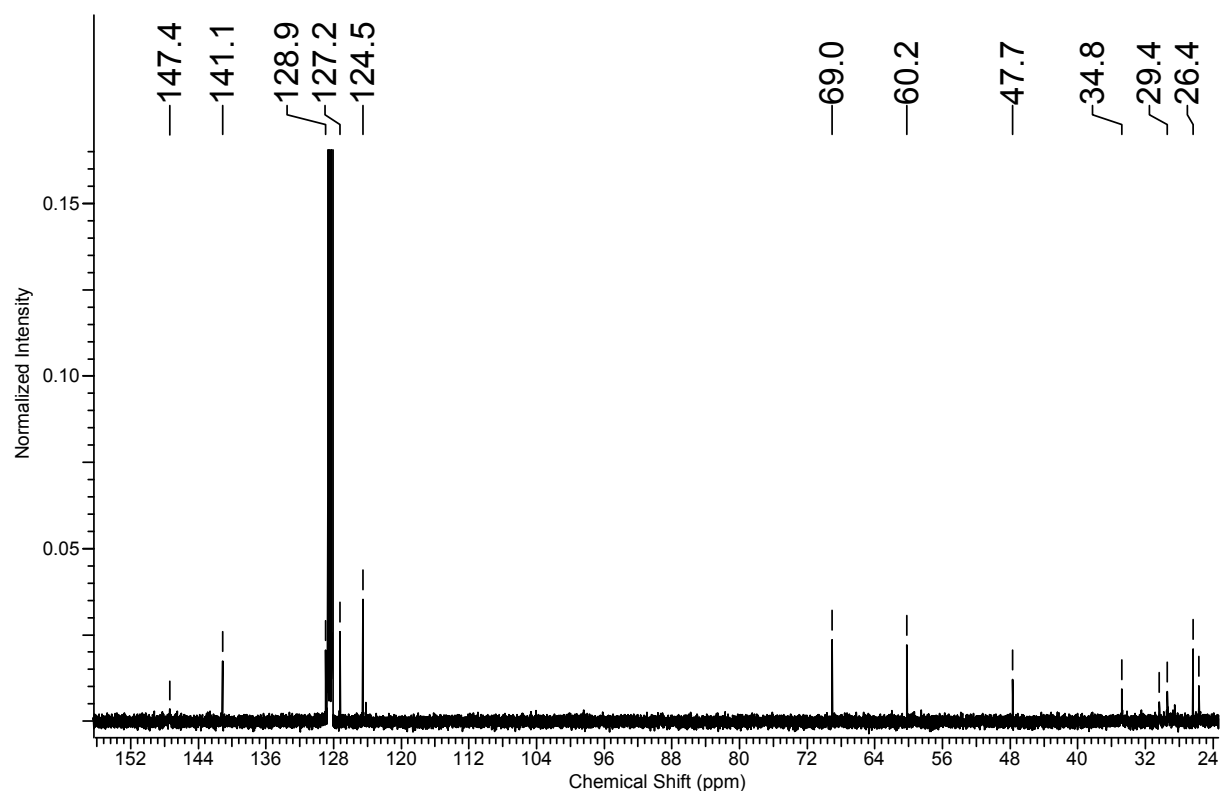


Figure S6. ^{11}B NMR spectrum of **3**-CAAC^{M_e} in C₆D₆.

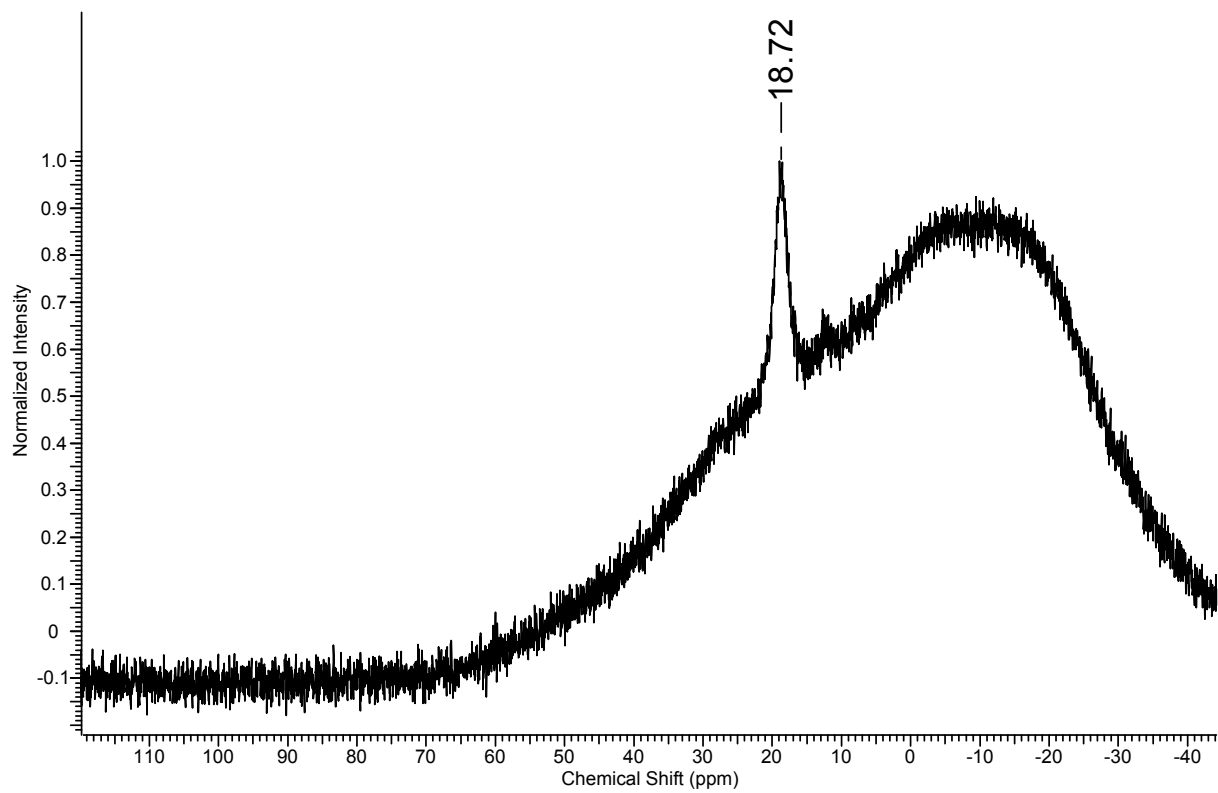


Figure S7. ^1H NMR spectrum of **3-IMes** in C_6D_6 .

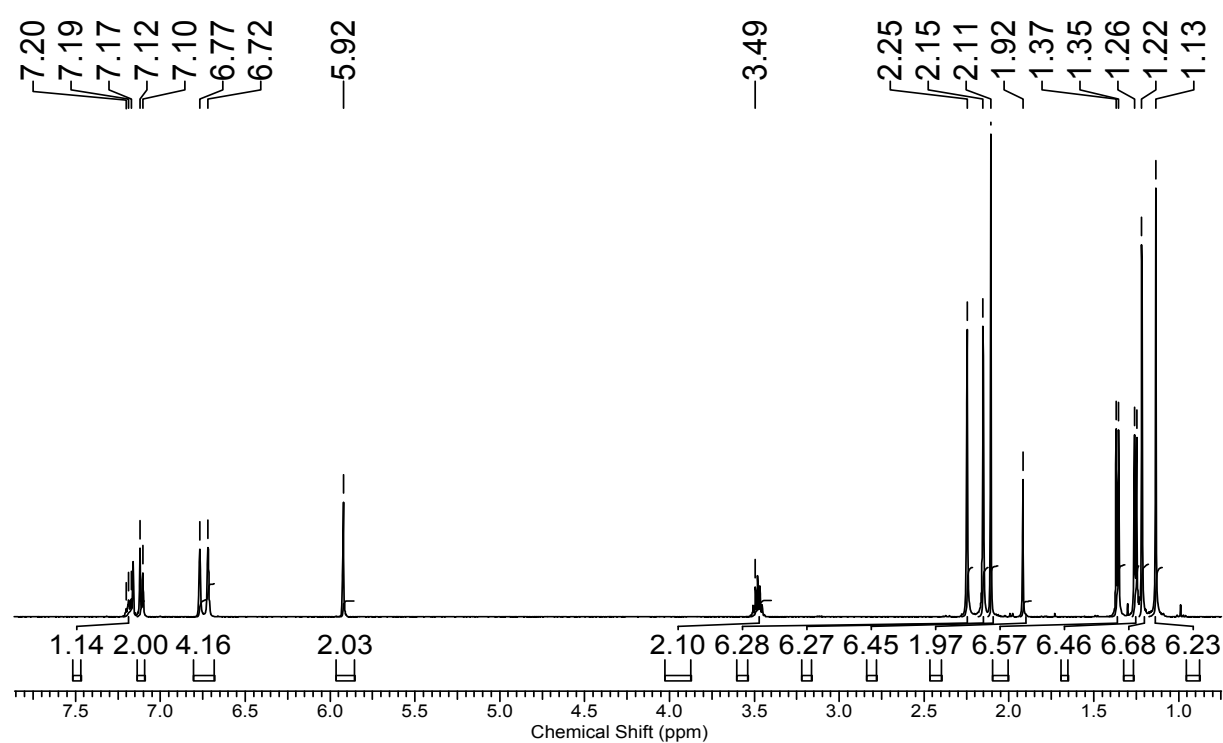


Figure S8. $^{13}\text{C}\{^1\text{H}\}$ NMR spectrum of **3-IMes** in C_6D_6 .

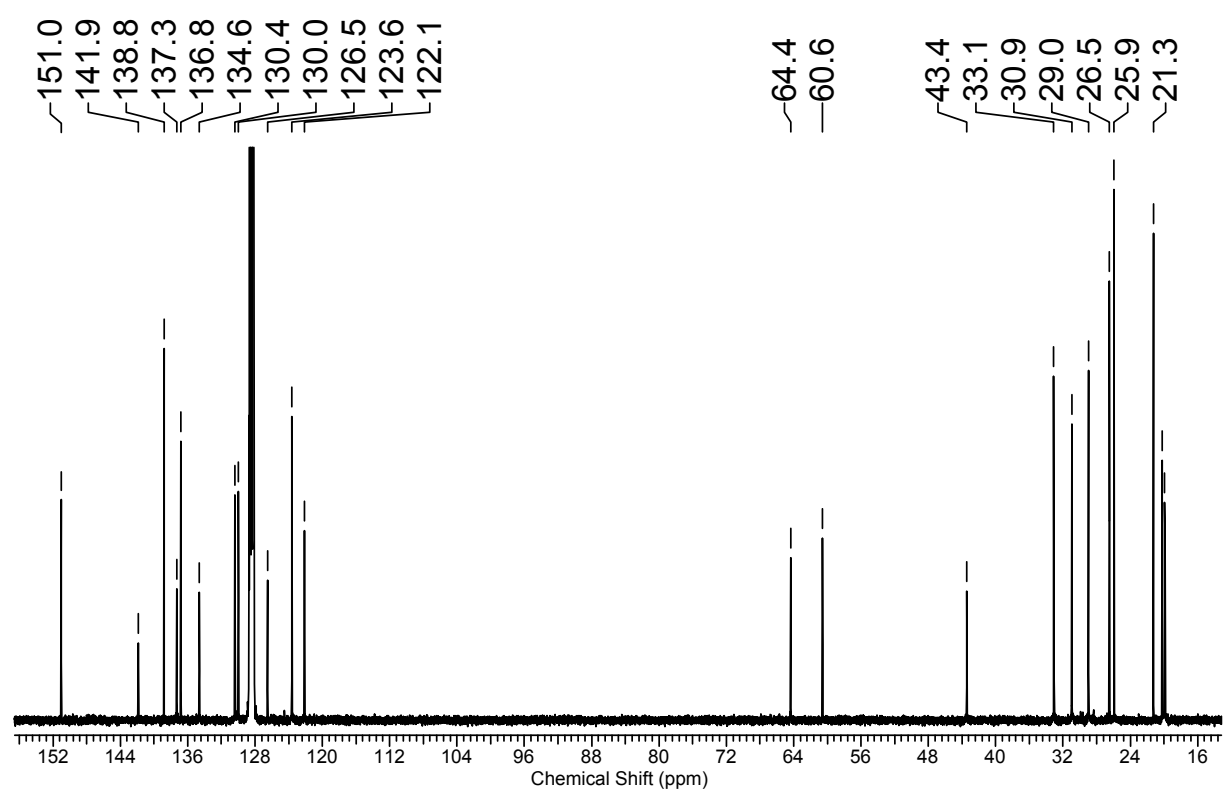


Figure S9. ^{11}B NMR spectrum of **3-IMes** in C_6D_6 .

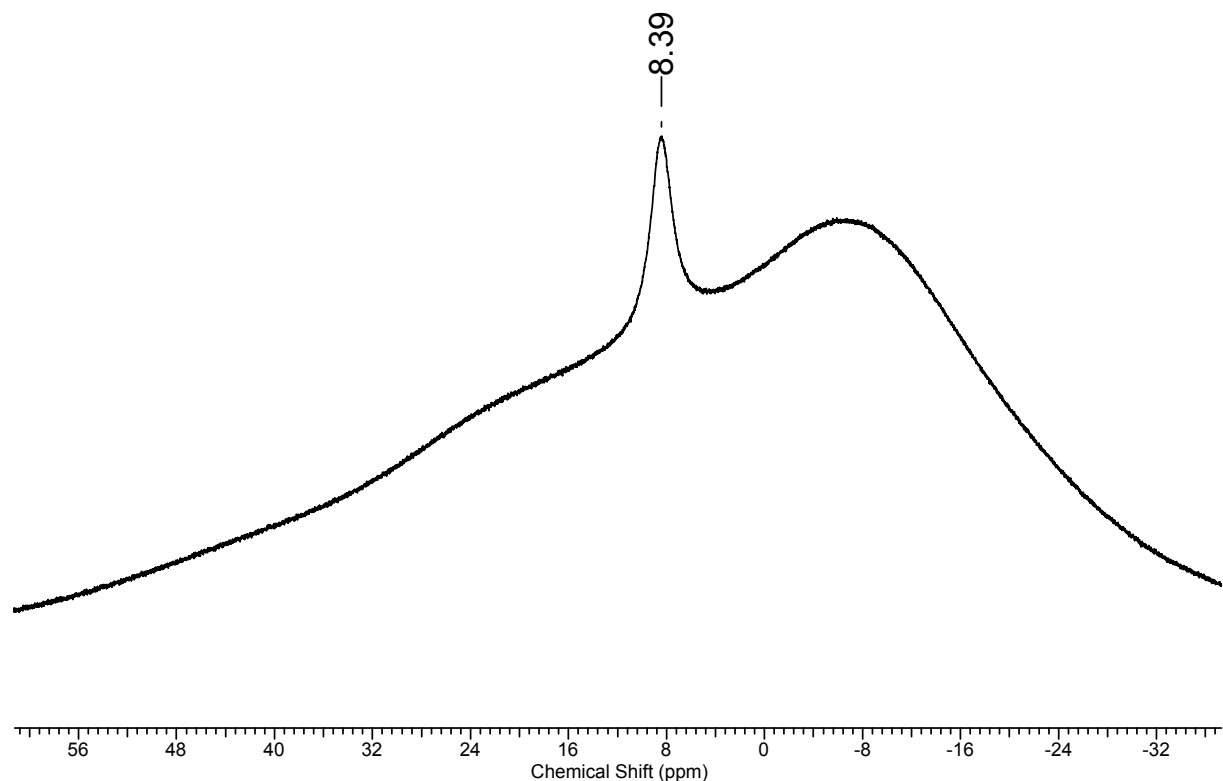


Figure S10. ^1H NMR spectrum of **3-SIMes** in C_6D_6 .

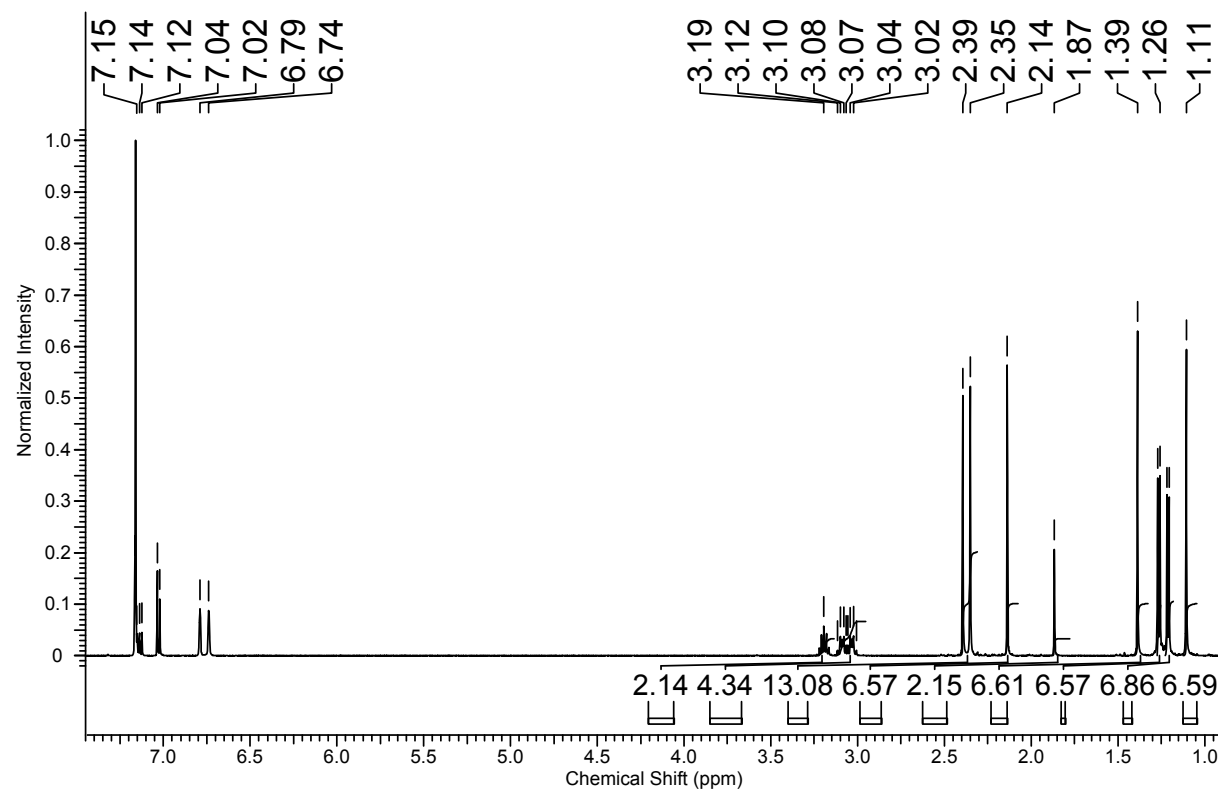


Figure S11. $^{13}\text{C}\{^1\text{H}\}$ NMR spectrum of **3-SIMes** in C_6D_6 . The additional small resonances at 34.8, 23.1 and 14.6 ppm correspond to residual hexane, those at 32.3, 23.4 and 14.7 ppm to residual pentane used for crystallisation.

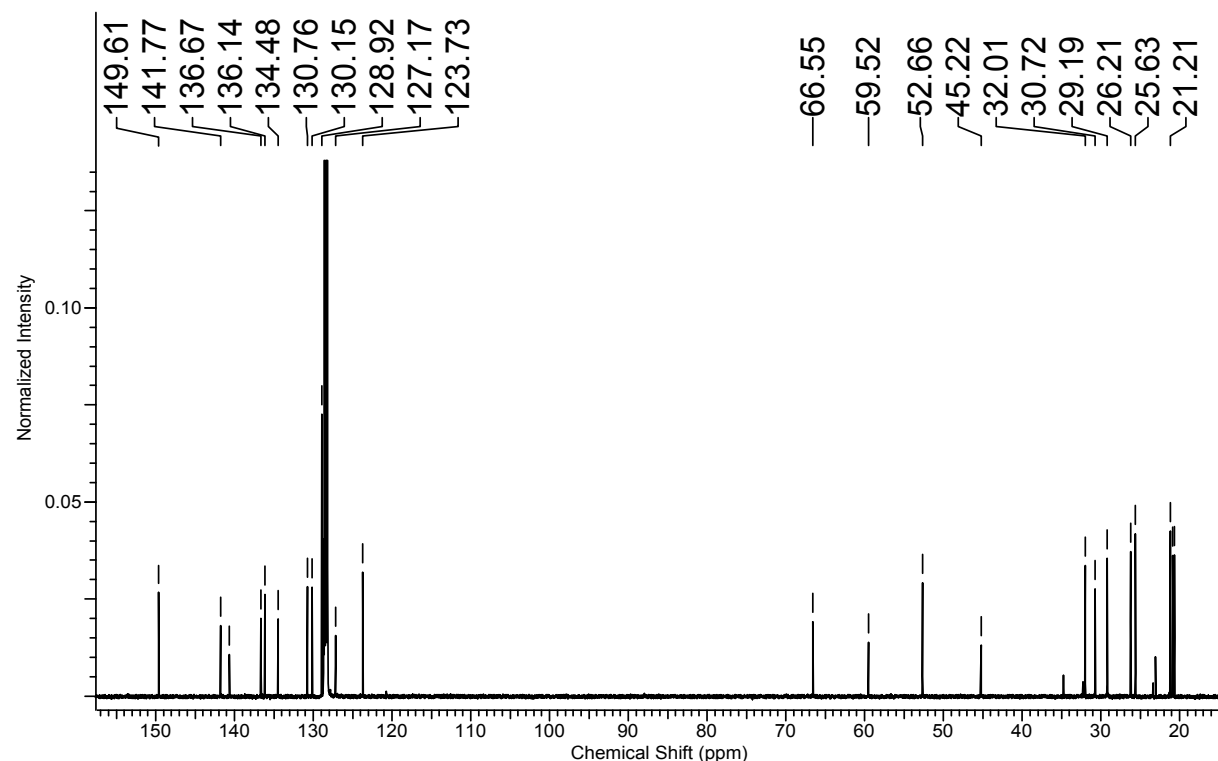


Figure S12. ^{11}B NMR spectrum of **3-SIMes** in C_6D_6 .

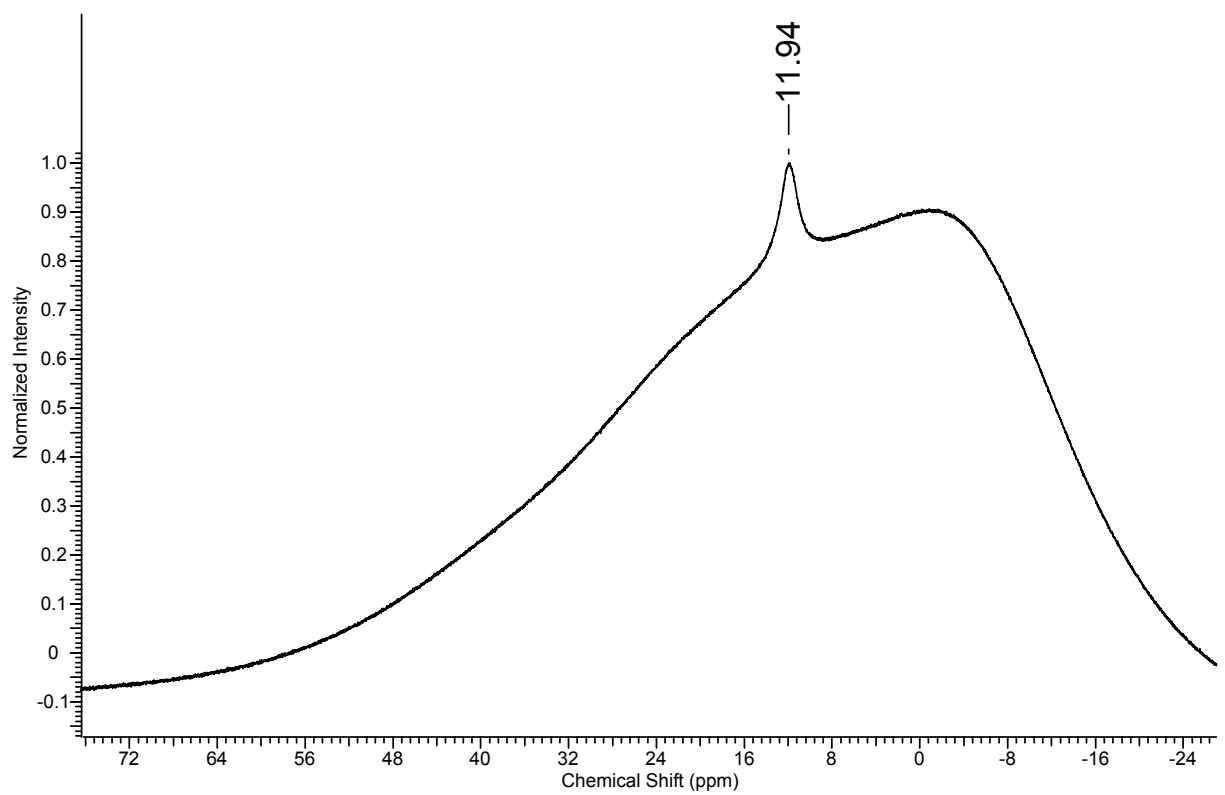


Figure S13. ^1H NMR spectrum of **3-PEt₃** in C₆D₆.

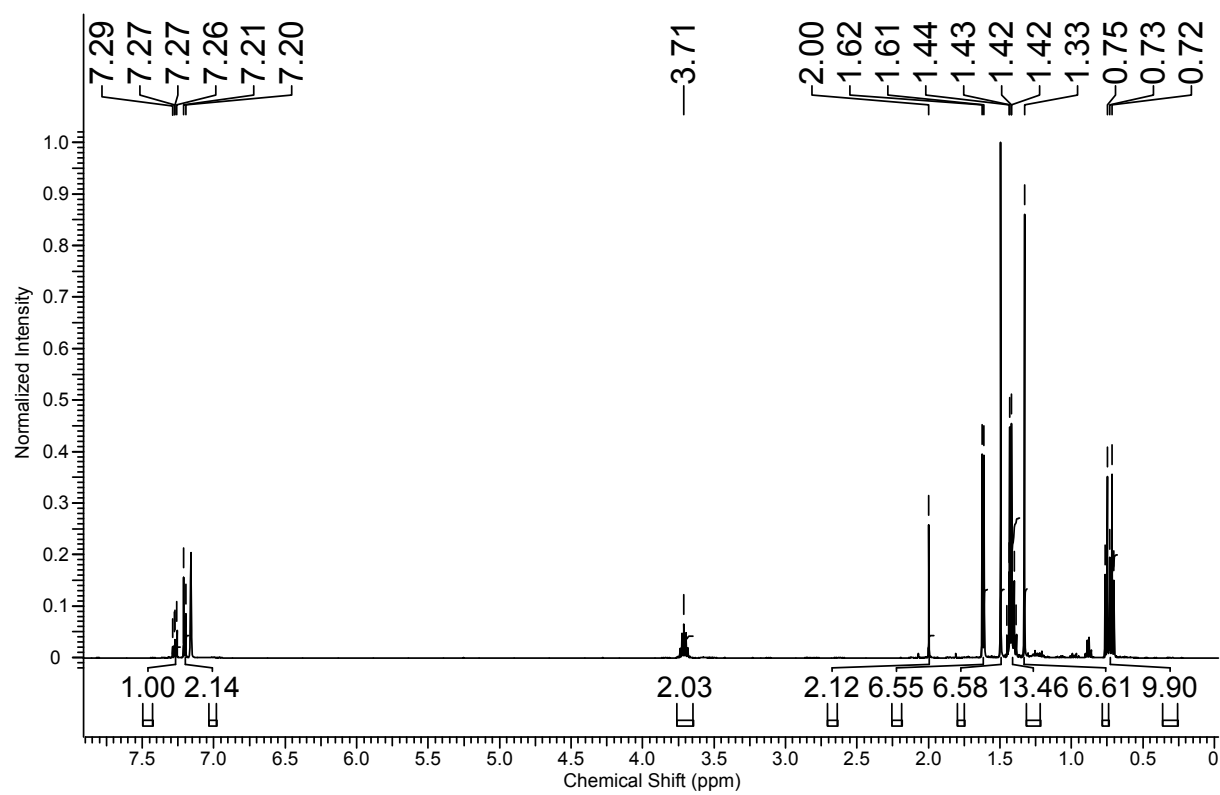


Figure S14. $^{13}\text{C}\{\text{H}\}$ NMR spectrum of **3-PEt₃** in C₆D₆.

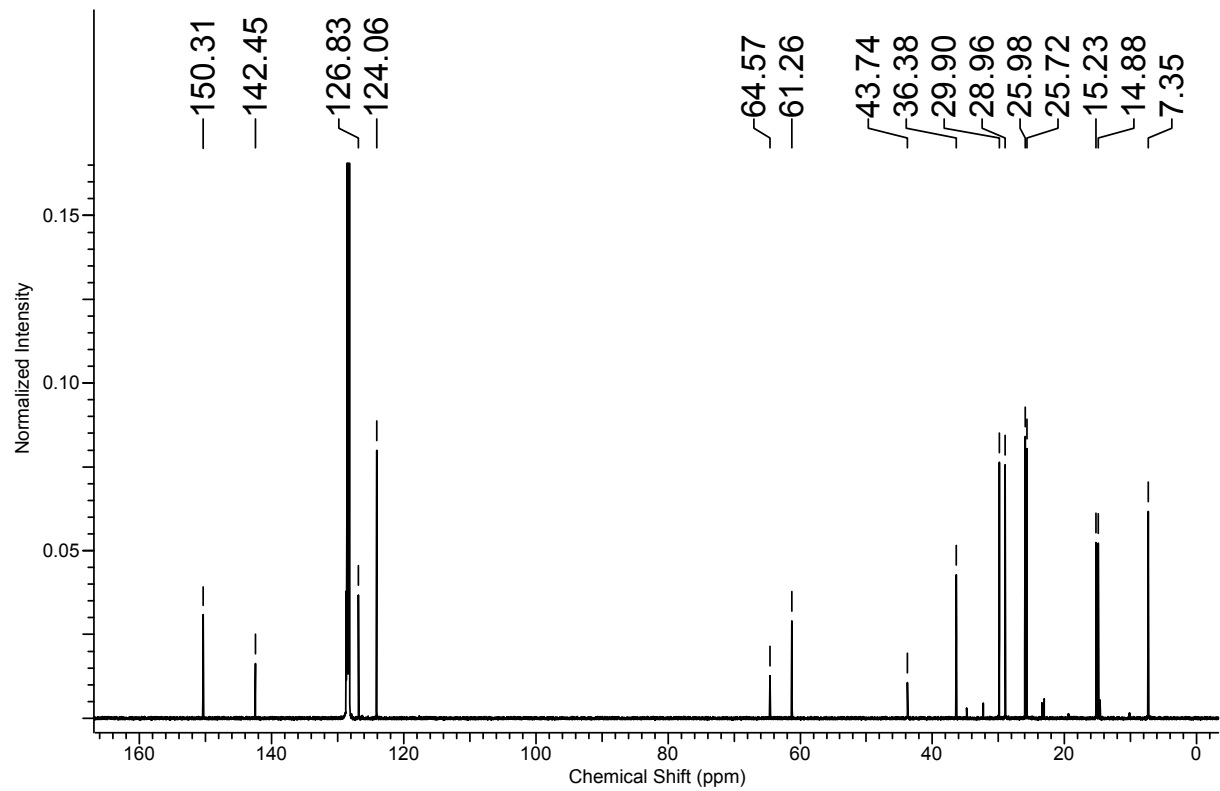


Figure S15. ^{11}B NMR spectrum of **3-PEt₃** in C₆D₆.

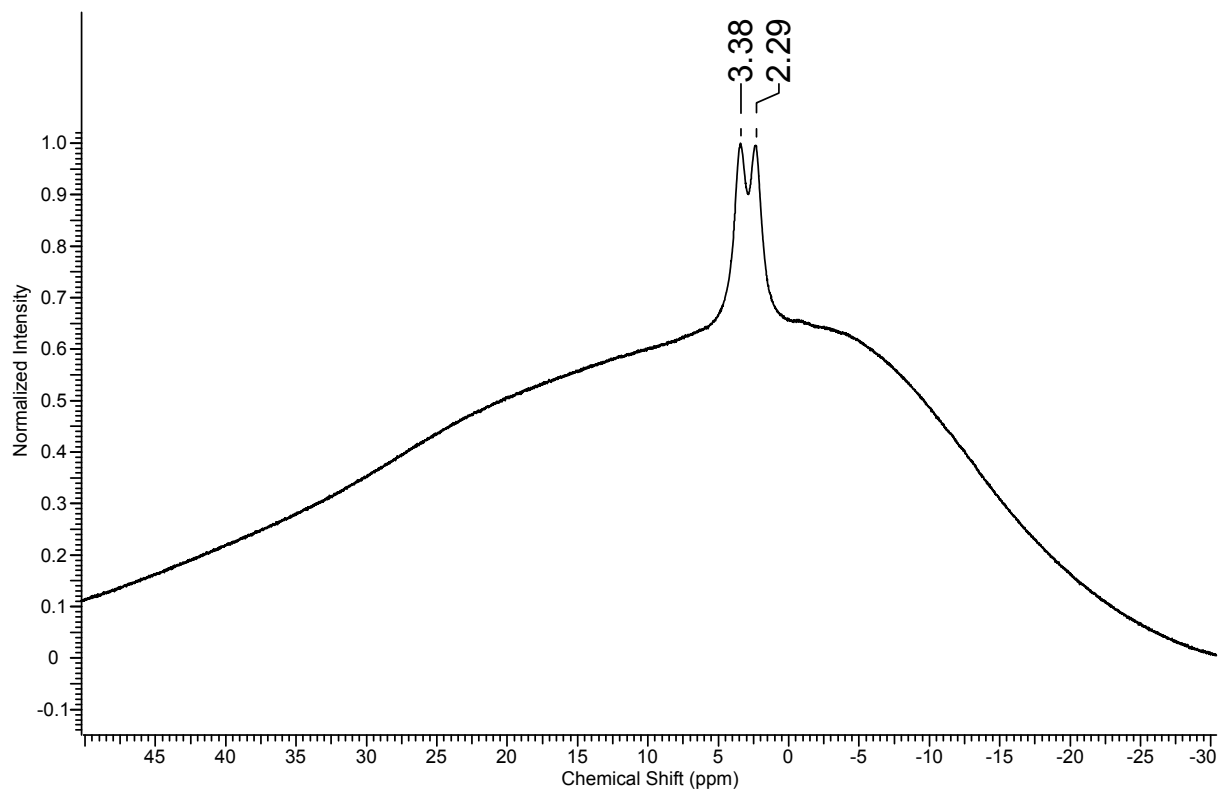


Figure S16. ^{31}P NMR spectrum of **3-PEt₃** in C₆D₆.

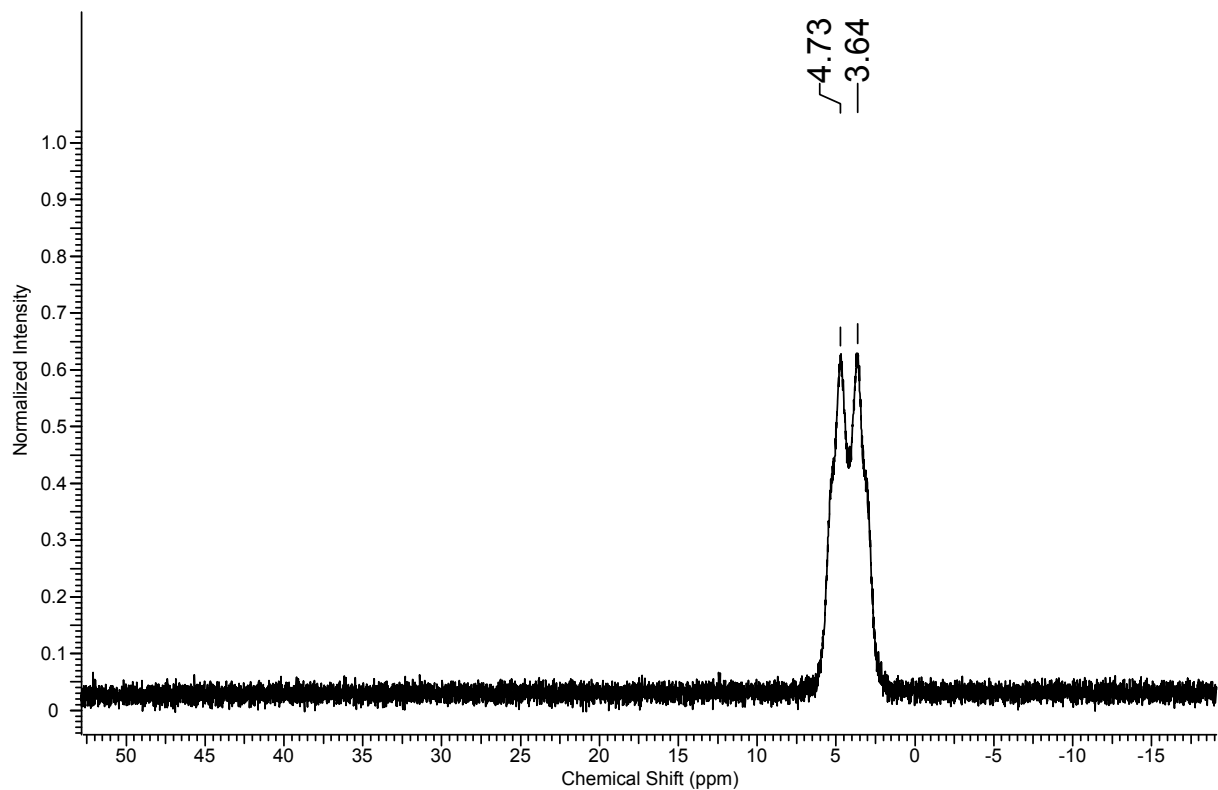


Figure S 17. ^1H NMR spectrum of **3-PMe₃** in C₆D₆.

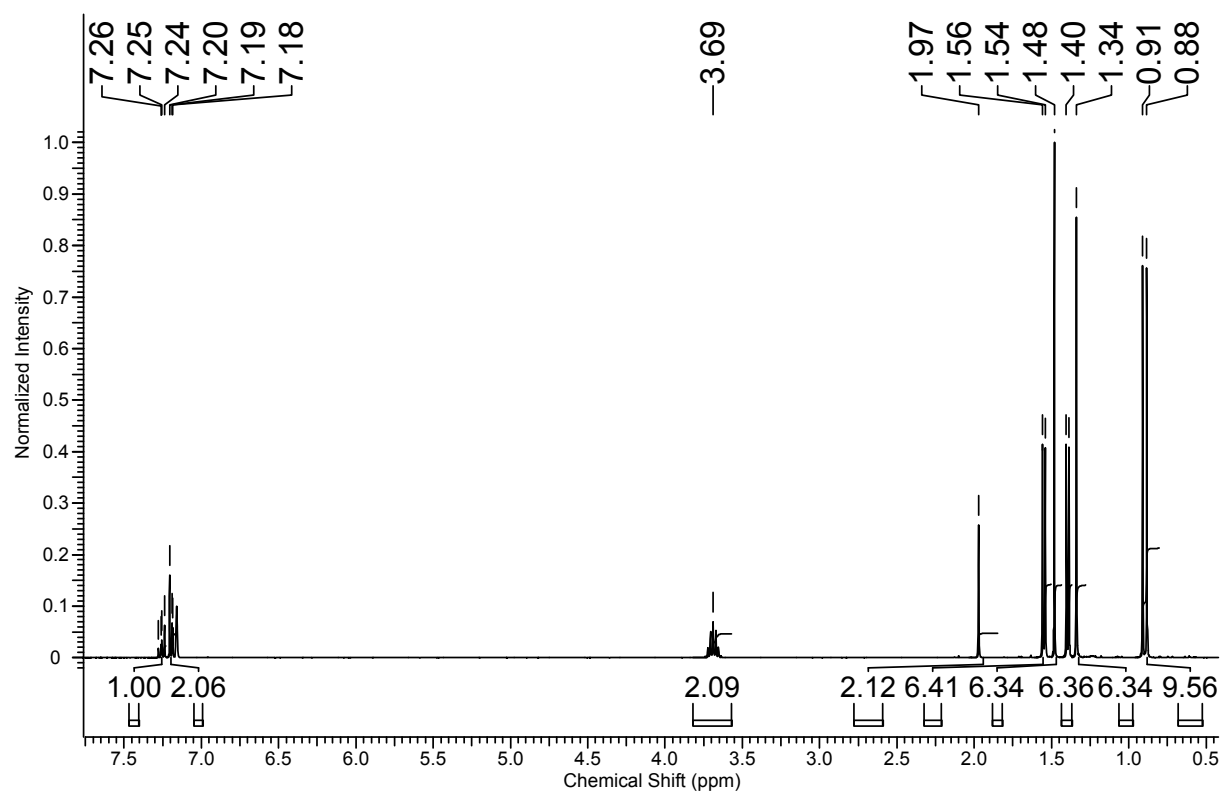


Figure S18. $^{13}\text{C}\{\text{H}\}$ NMR spectrum of **3-PMe₃** in C₆D₆.

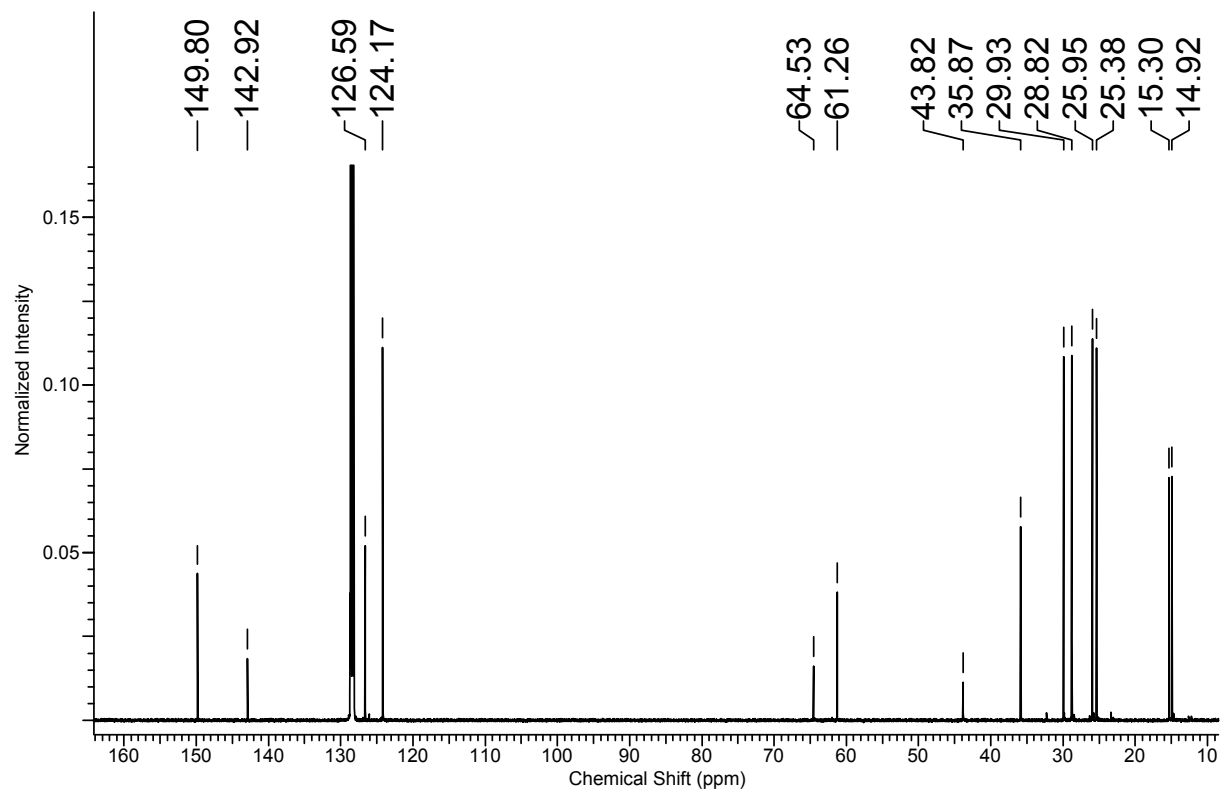


Figure S19. ^{11}B NMR spectrum of **3-PMe₃** in C₆D₆.

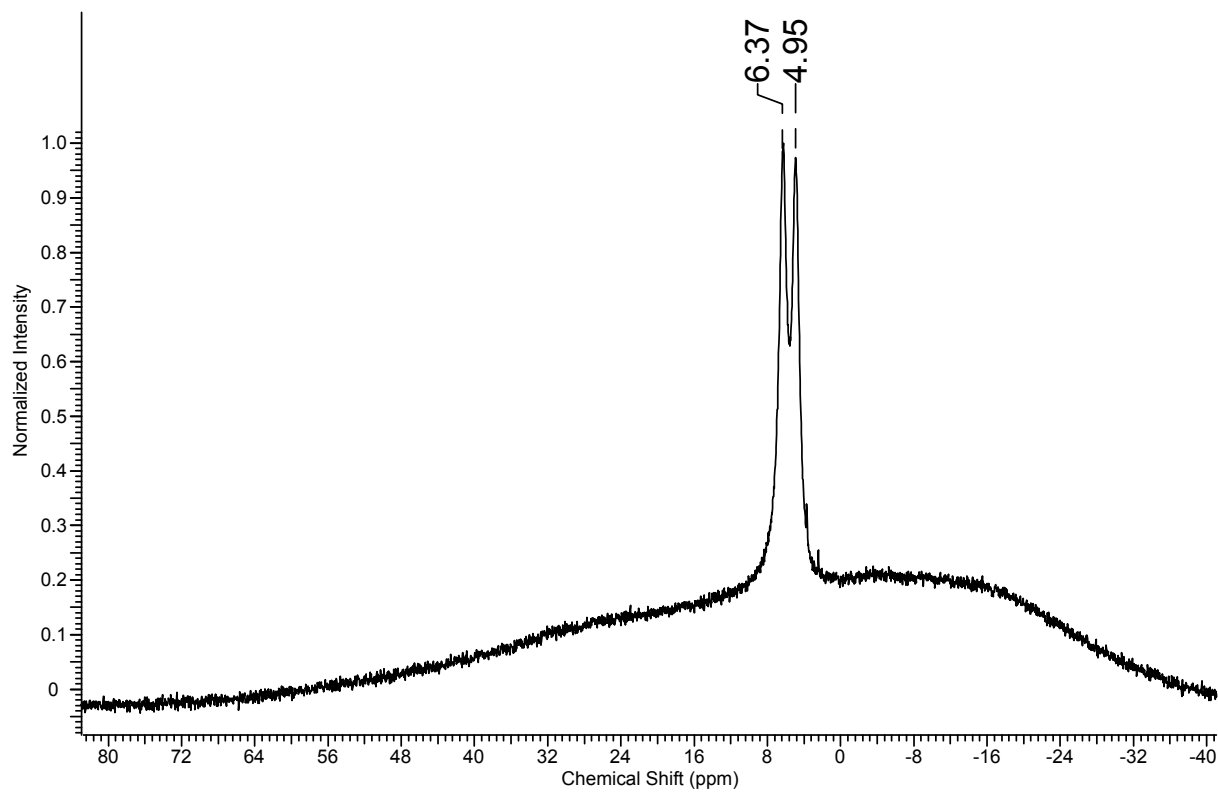


Figure S20. ^{31}P NMR spectrum of **3-PMe₃** in C₆D₆.

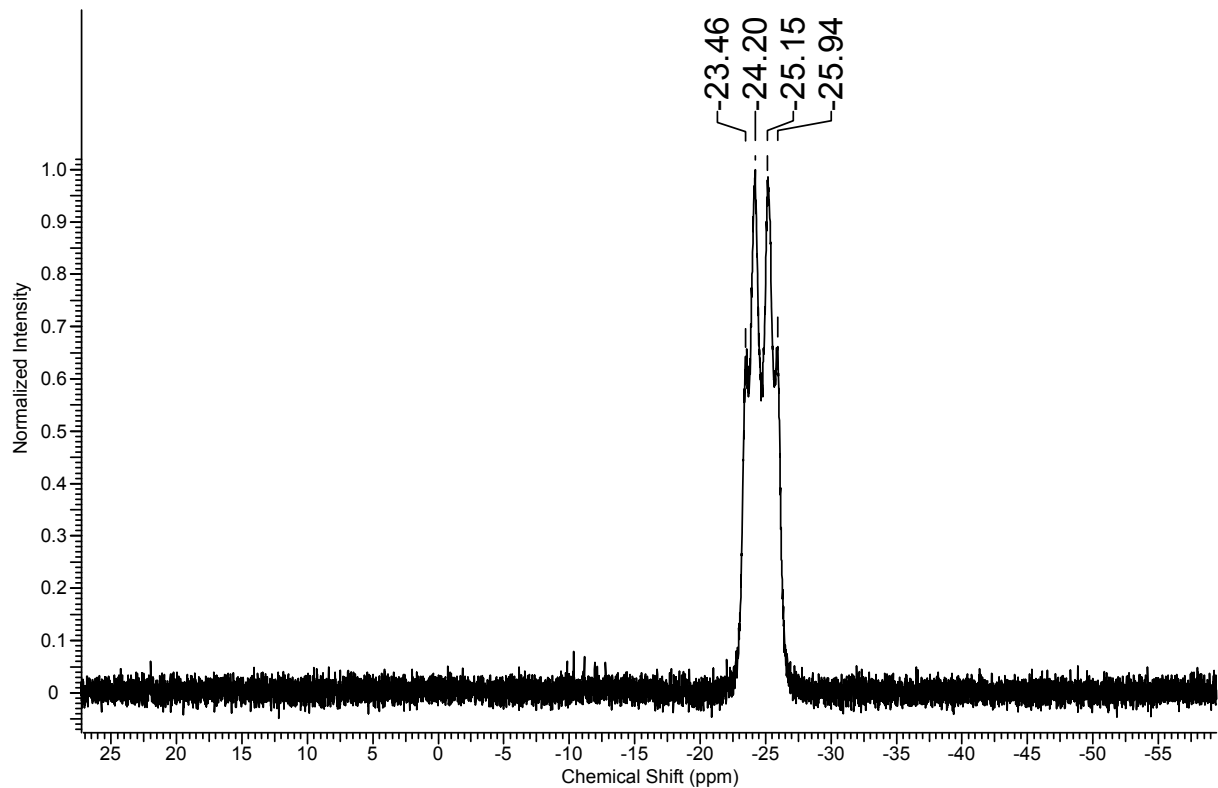


Figure S21. ^1H NMR spectrum of **3-IMe^{Me}** in C_6D_6 .

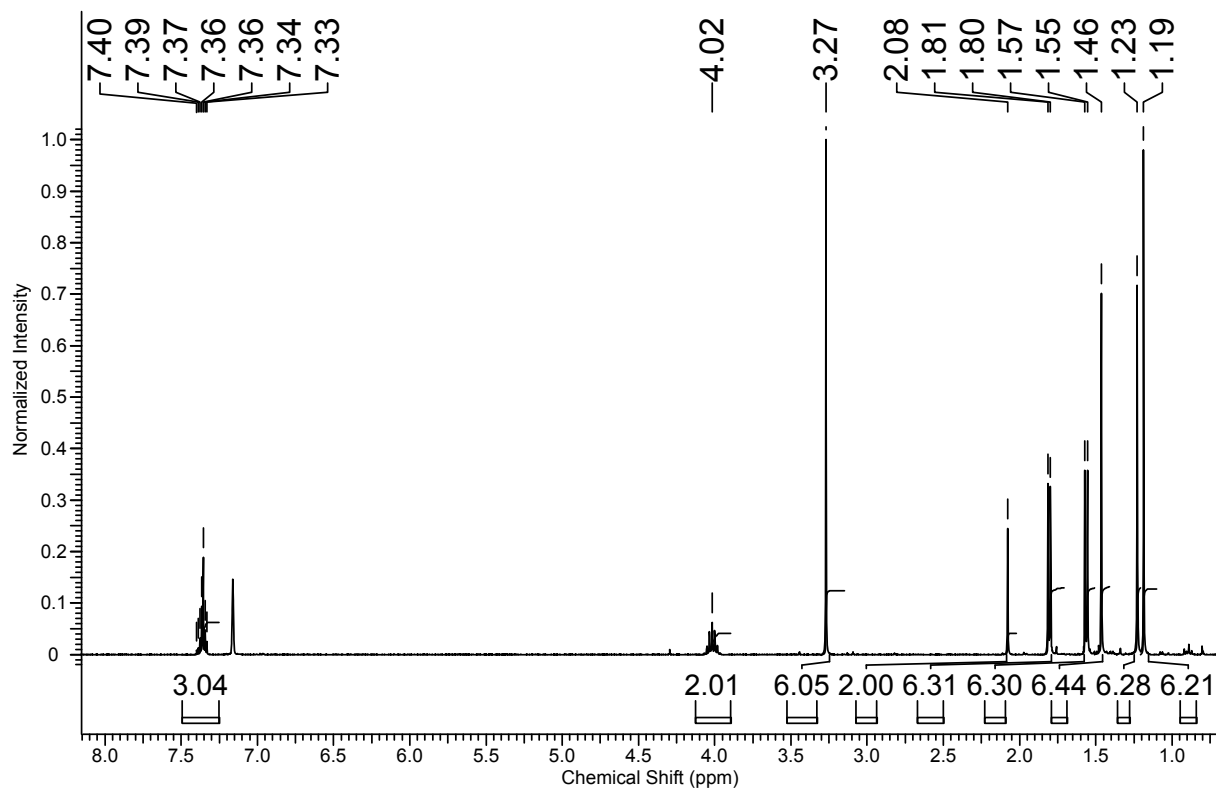


Figure S22. $^{13}\text{C}\{^1\text{H}\}$ NMR spectrum of **3-IMe^{Me}** in C_6D_6 .

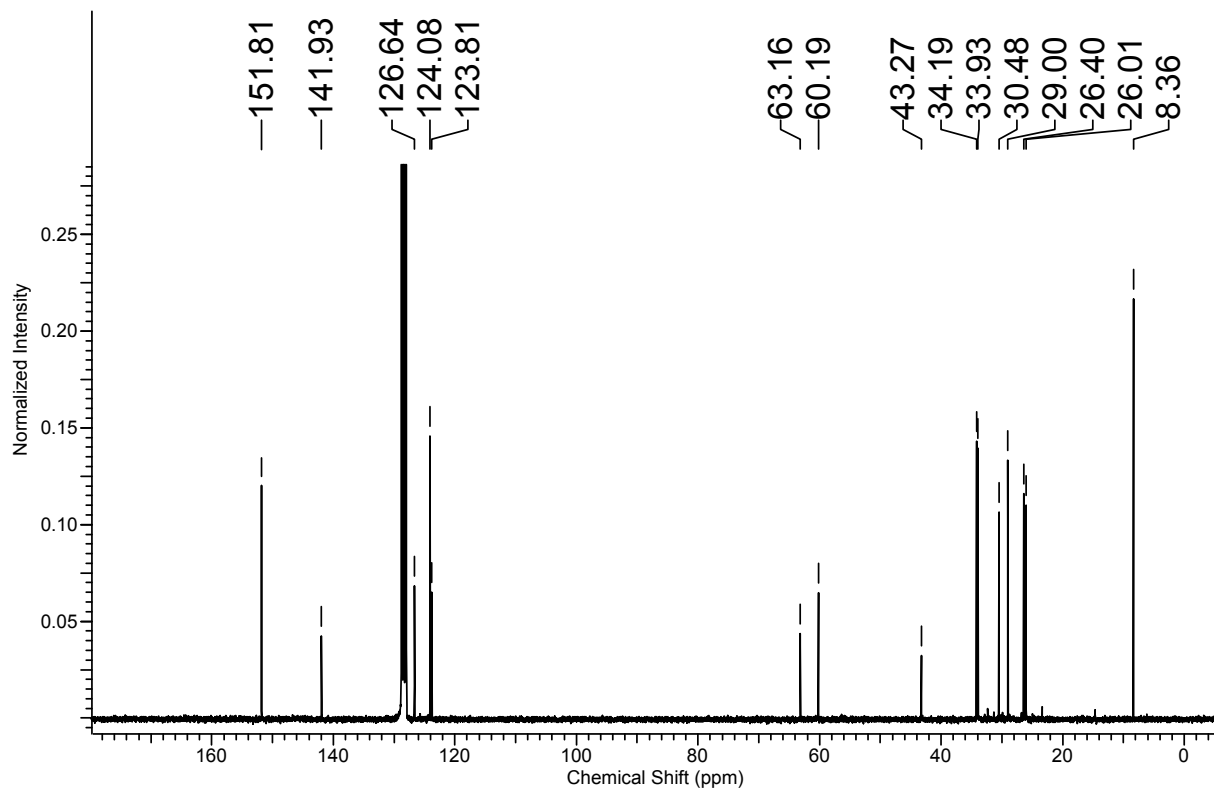


Figure S23. ^{11}B NMR spectrum of **3-IMe^{Me}** in C₆D₆.

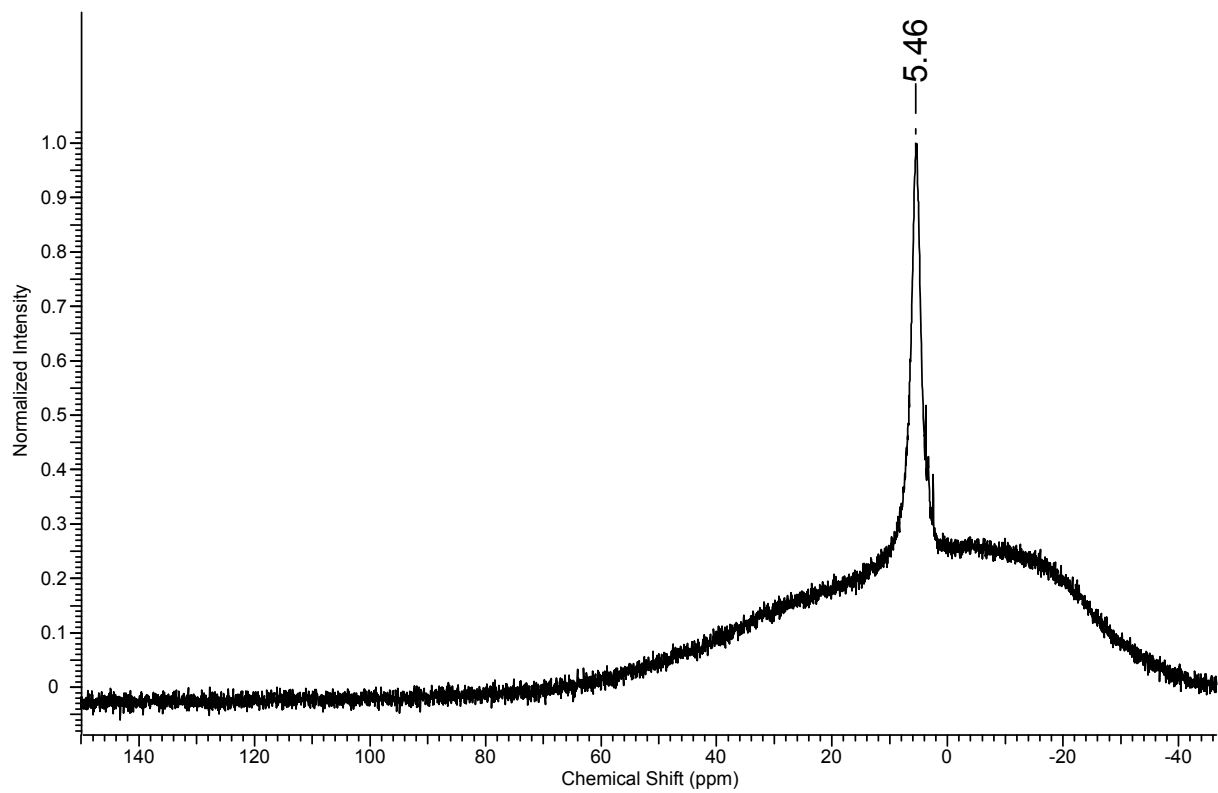


Figure S24. ^{11}B NMR spectrum of isolated crystals of **6** directly dissolved in protio-THF.

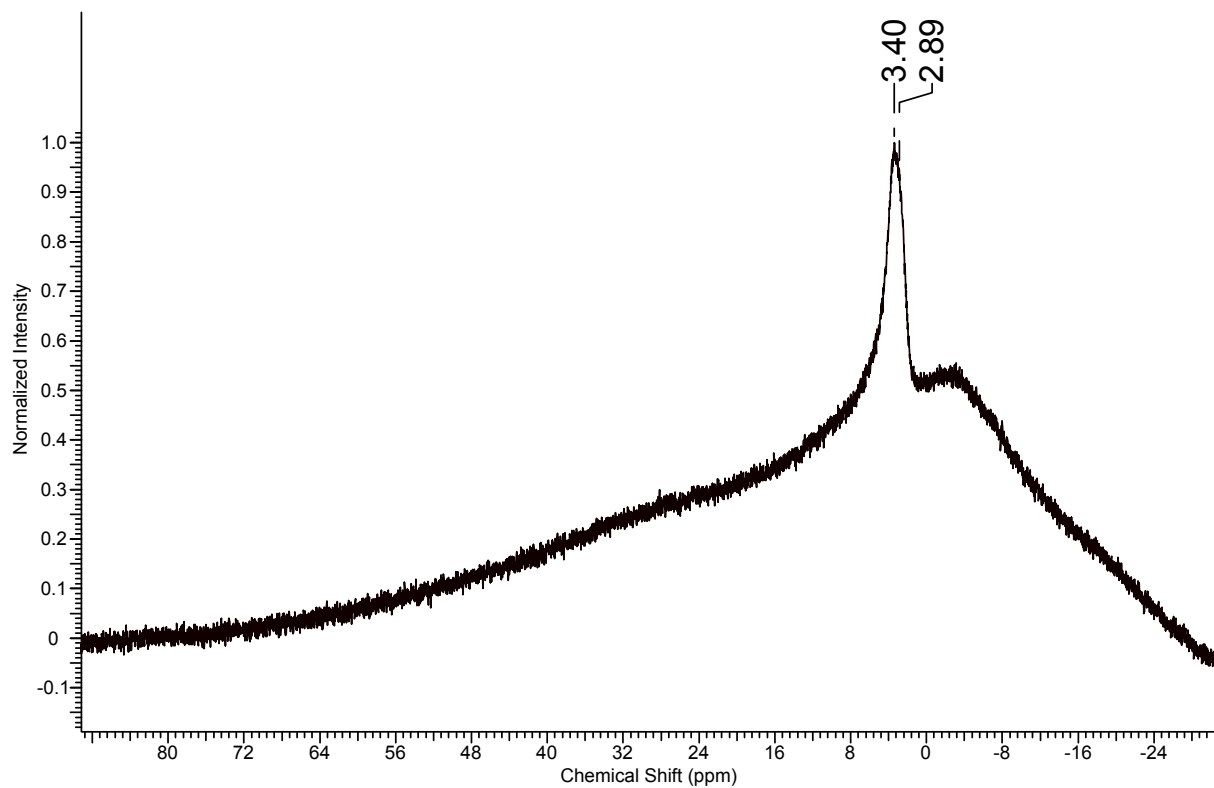


Figure S25. ^{11}B NMR spectrum of isolated crystals of **6** dried in vacuo and dissolved in C_6D_6 . The new doublet centred at 1.2 ppm corresponds to the hydrolysis byproduct **5-IMes**.

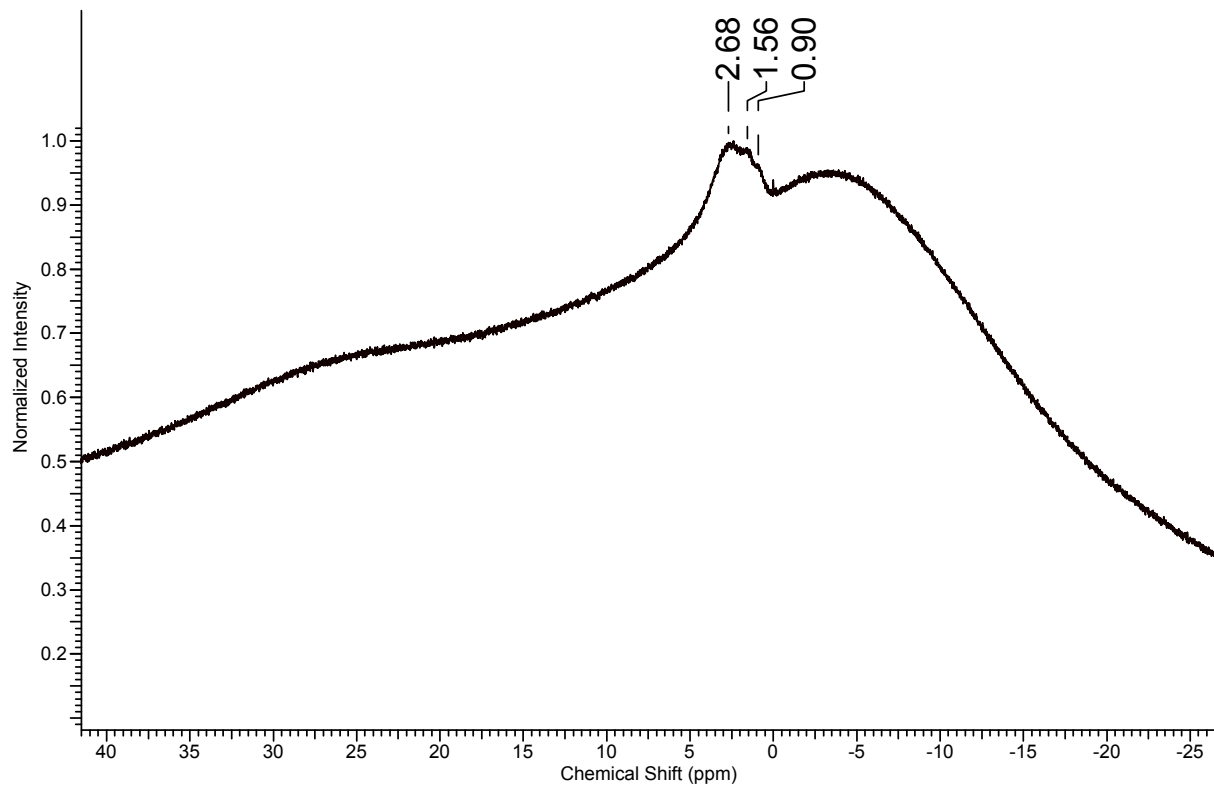


Figure S26. ^1H NMR spectrum of **6** (ca. 80%, marked with ♦) in C_6D_6 . The hydrolysis byproduct **5-IMes** (ca., 20%) is marked with ●.

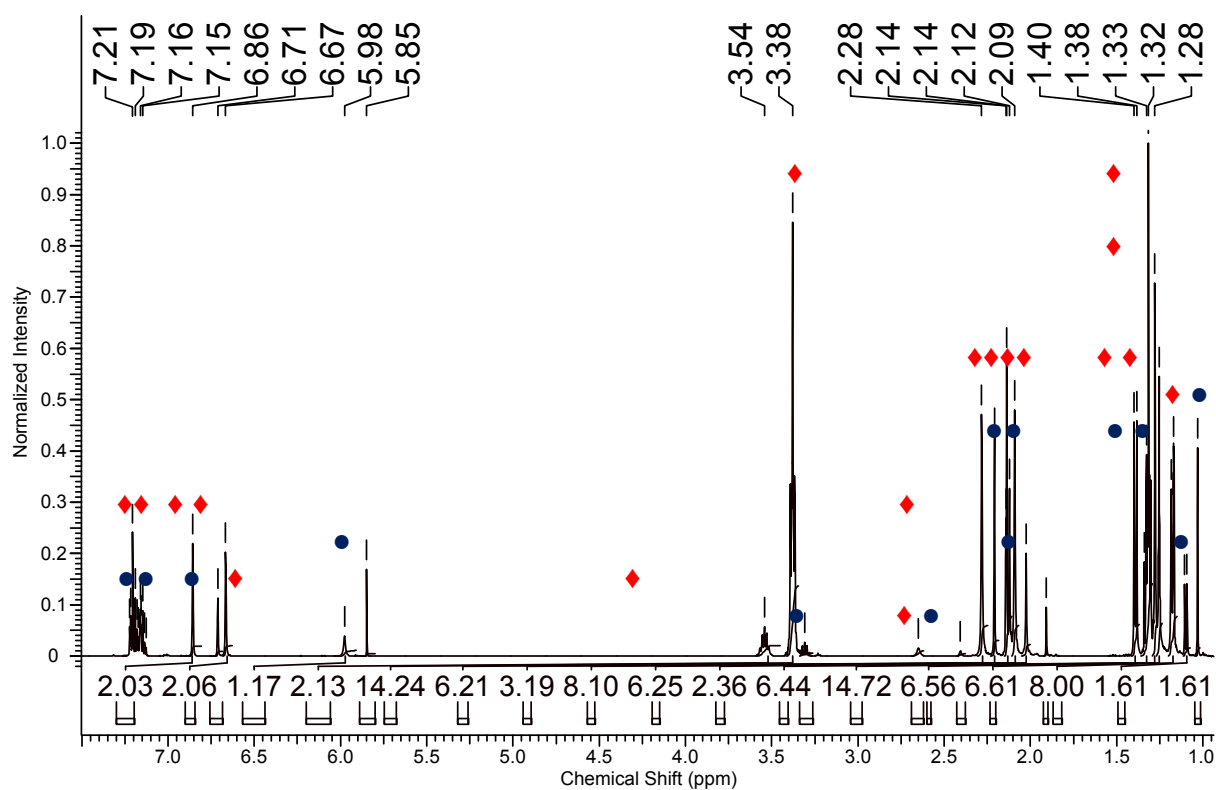


Figure S27. $^{13}\text{C}\{\text{H}\}$ NMR spectrum of **6** (ca. 80% purity) in C_6D_6 .

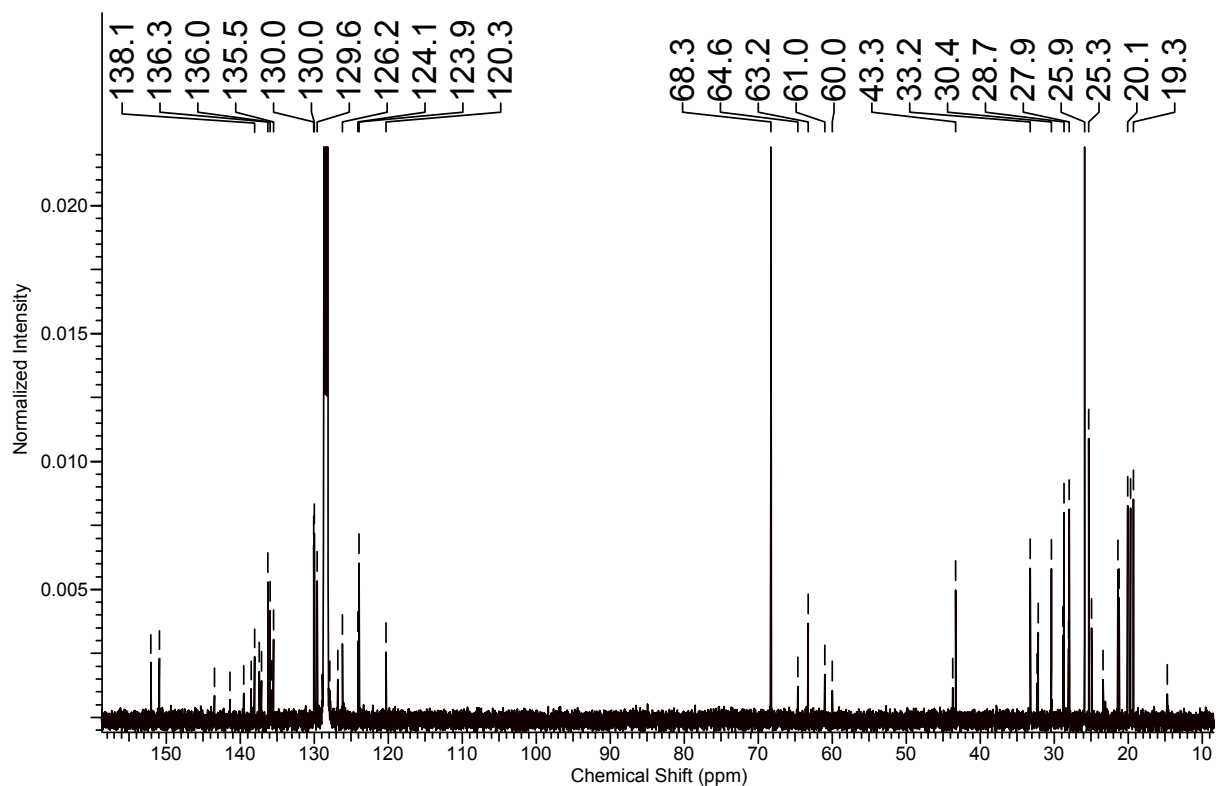


Figure S28. ^1H NMR spectrum of **5-IMes** in C_6D_6 .

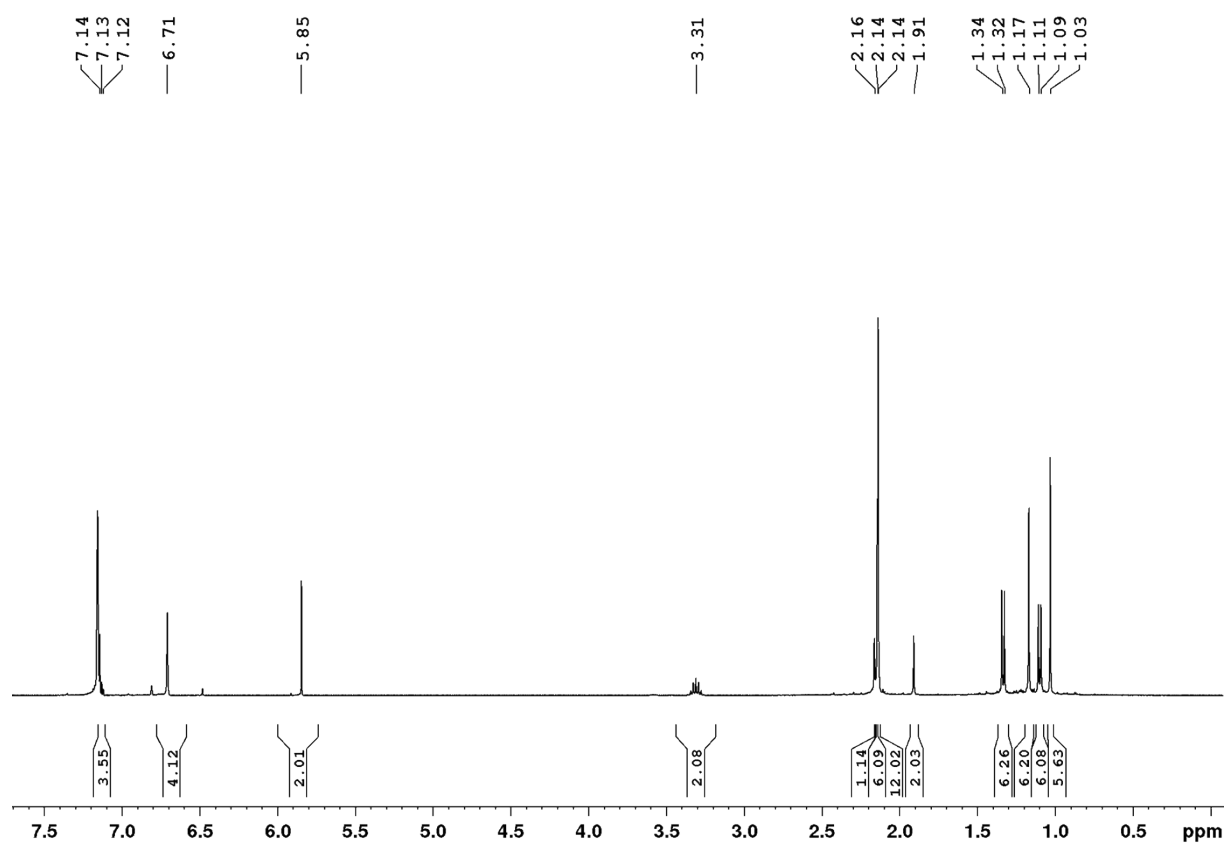


Figure S29. $^{13}\text{C}\{\text{H}\}$ NMR spectrum of **5-IMes** in C_6D_6 .

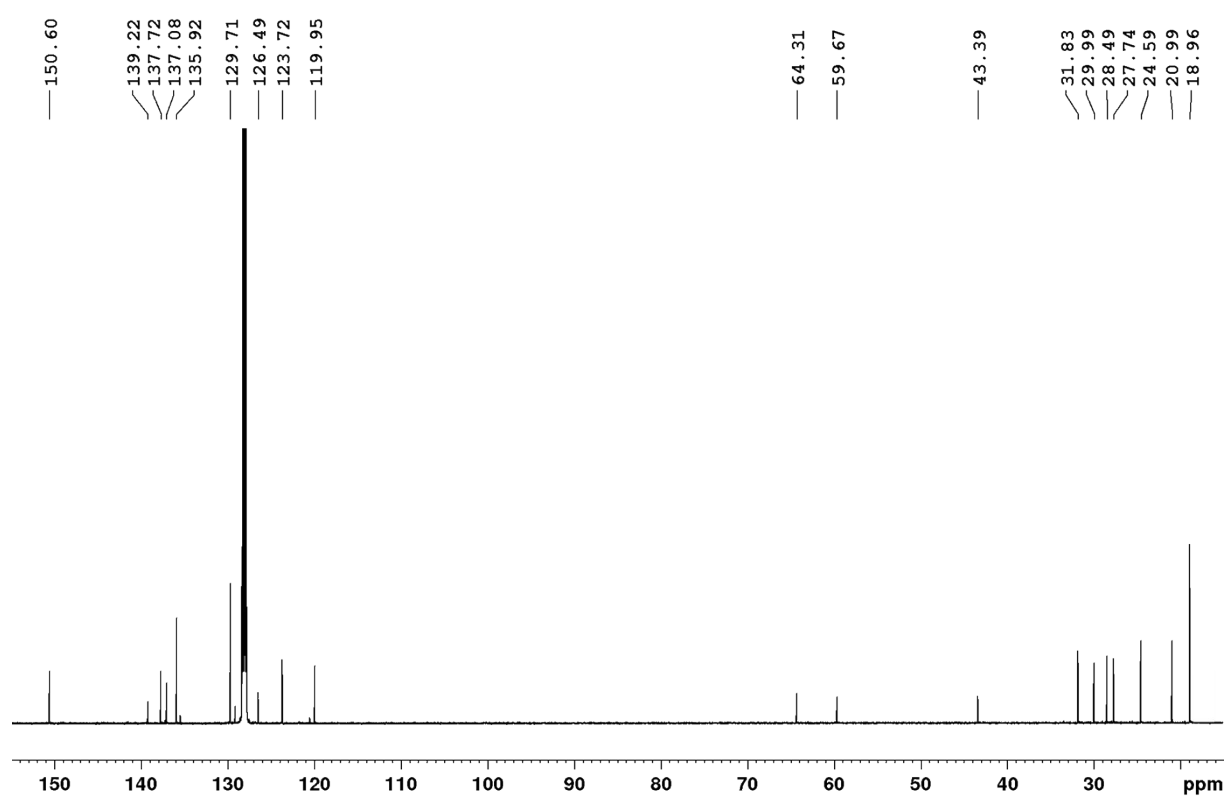
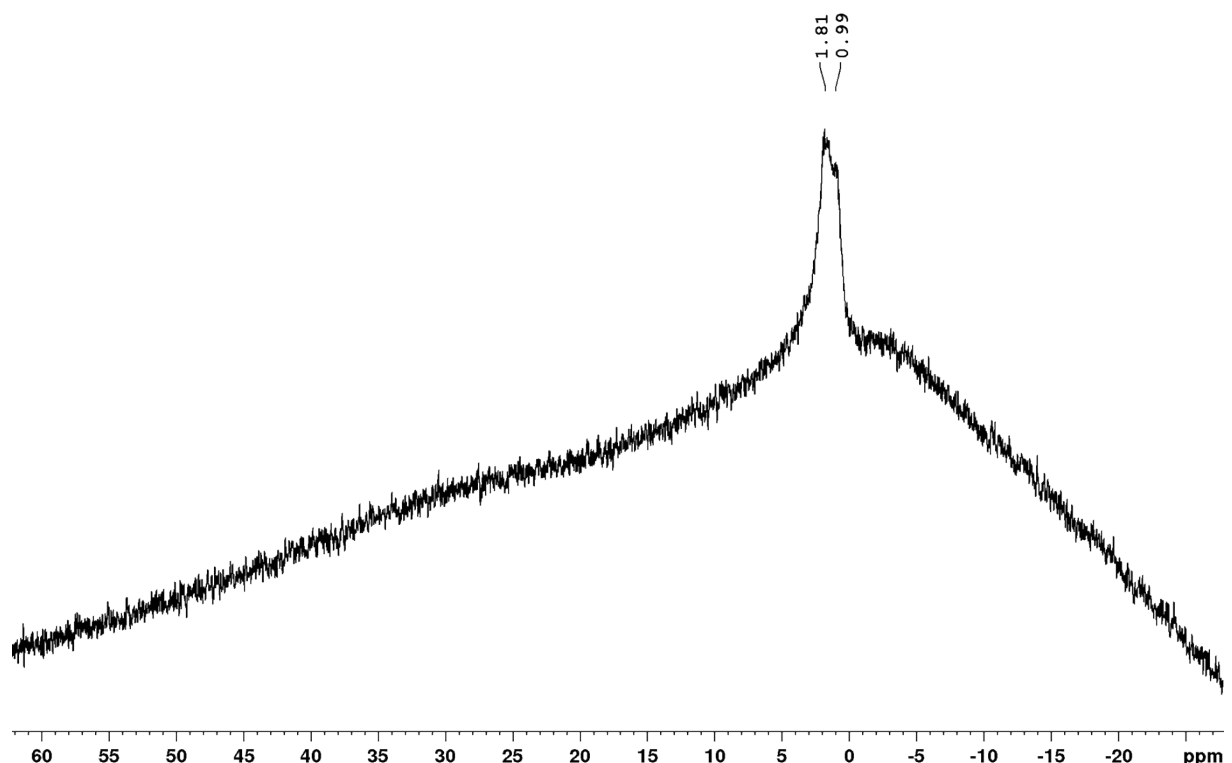


Figure S30. ^{11}B NMR spectrum of **5-IMes** in C_6D_6 .



EPR spectrum of radical 2

CW EPR measurements at X-band were carried out using a Bruker ELEXSYS E580 EPR spectrometer. The spectrum of **2** was taken at room temperature with a modulation amplitude of 1 G and a microwave power of 0.6 mW. The symmetrical EPR signal is broad with a peak-to-peak linewidth of ca. 2 mT. Possible hyperfine splittings from the chloride nuclei are not resolved because of the very low spin density on these atoms ($g_{\text{iso}} = 2.003$).

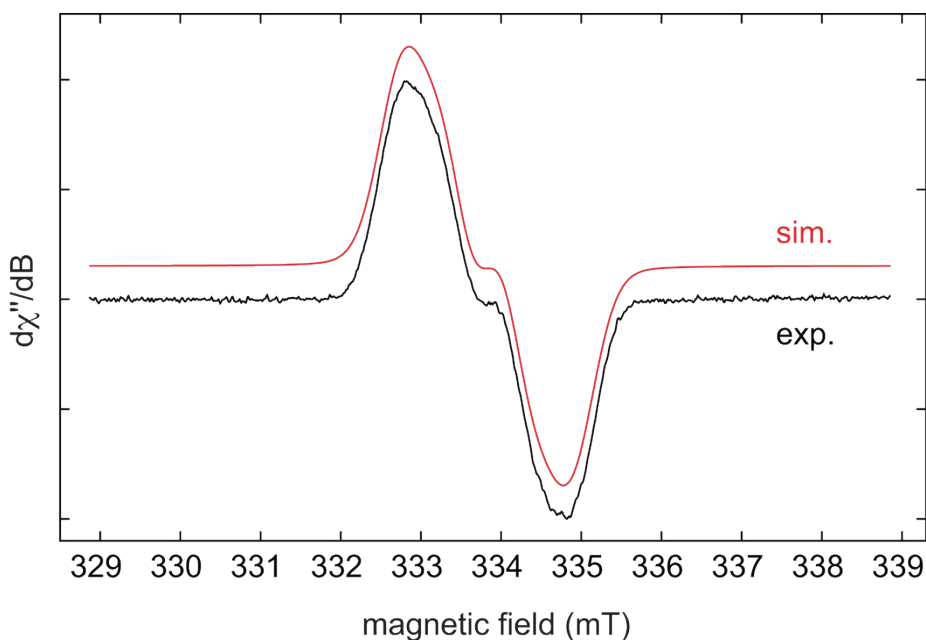


Figure S31. Experimental (black) and simulated (red) EPR spectrum of **2**. The best fit for the simulated spectrum was obtained using the following parameters: $a(^{14}\text{N}) = 17.3 \text{ MHz} (6.2 \text{ G})$ and $a(^{11}\text{B}) = 6.70 \text{ MHz} (2.4 \text{ G})$.

UV-vis spectra of compounds 2 and 3-L

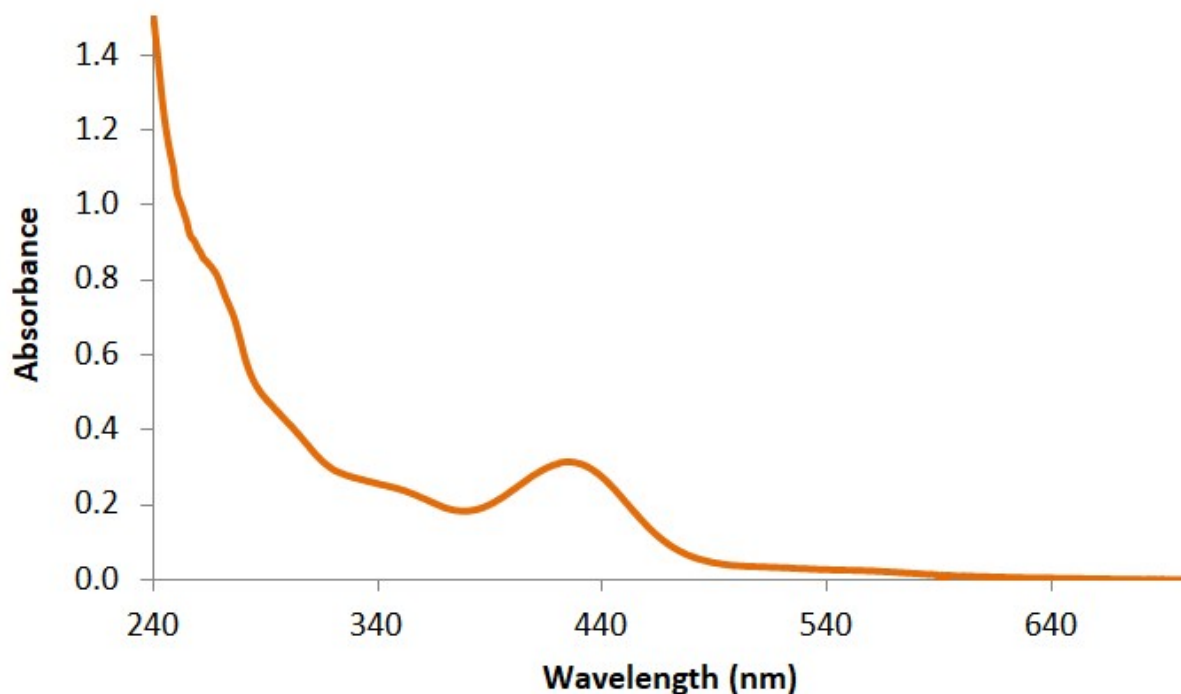


Figure S32. UV-vis spectrum of radical **2** in THF ($c \approx 0.1$ M).

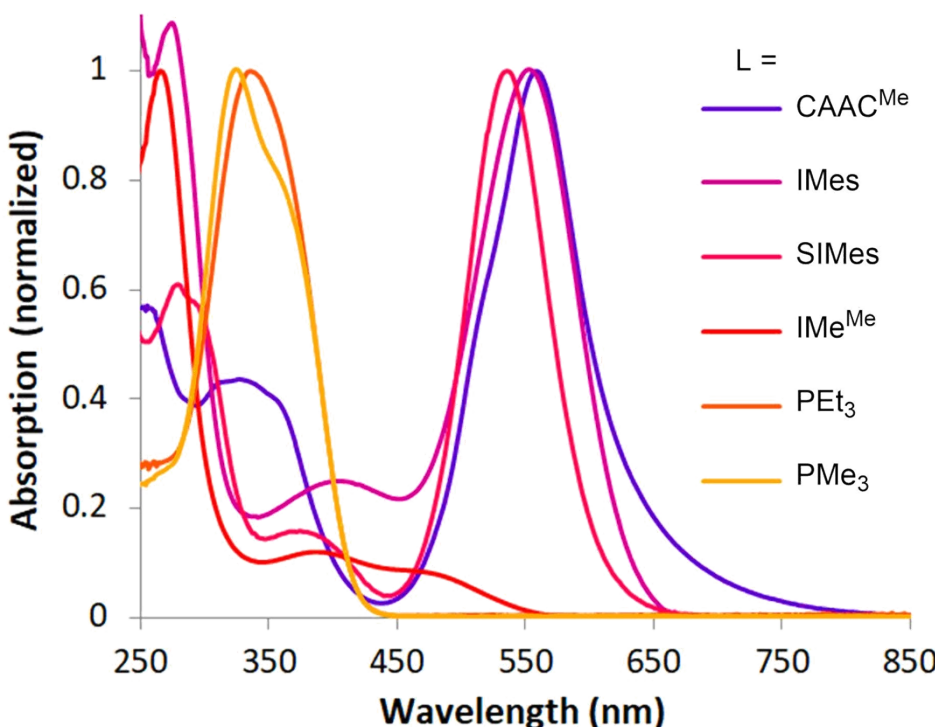


Figure S33. Overlay of the UV-vis spectra of the mixed-base borylenes **3-L** in THF, normalised to an absorbance maximum of 1.

Cyclic voltammetry

Cyclic voltammetry experiments were performed using a Gamry Instruments Reference 600 potentiostat. A standard three-electrode cell configuration was employed using a platinum disk working electrode, a platinum wire counter electrode, and a silver wire, separated by a *Vycor* tip, serving as the reference electrode. Formal redox potentials are referenced to the ferrocene/ferrocenium (Fc/Fc^+) redox couple. Tetra-*n*-butylammonium hexafluorophosphate ($[\text{nBu}_4\text{N}][\text{PF}_6]$) was employed as the supporting electrolyte. Compensation for resistive losses (iR drop) was employed for all measurements.

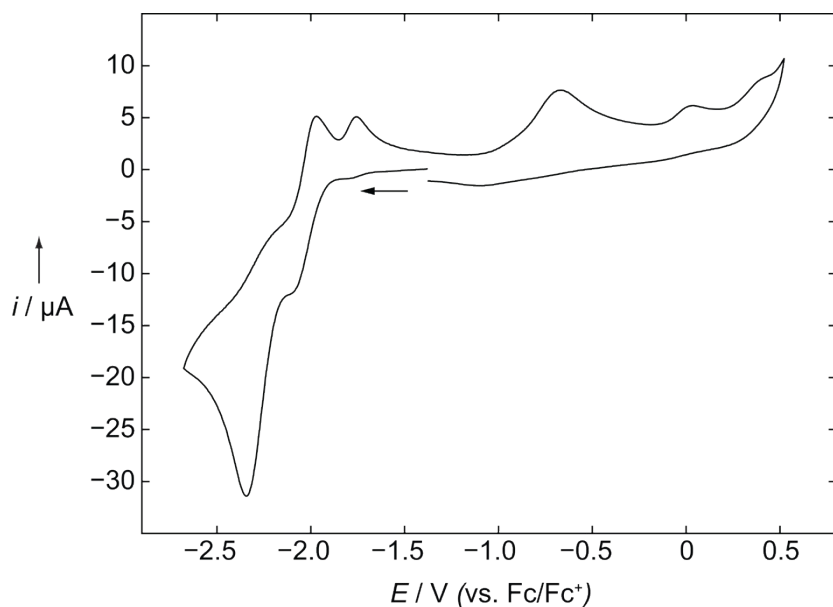


Figure S34. Cyclic voltammograms of **2** with different scan directions in THF. Formal potentials for reduction: $E_{\text{pc}} = -2.35 \text{ V}$ (irreversible).

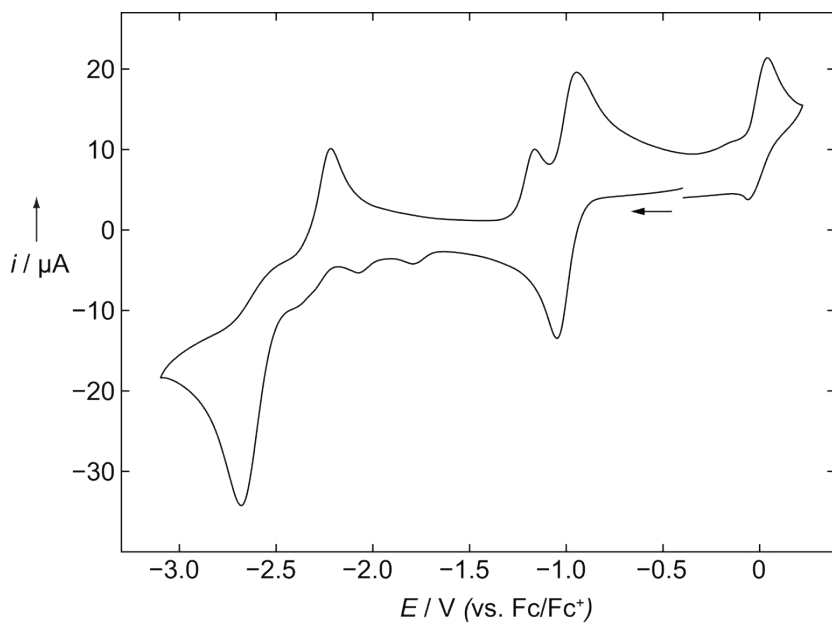


Figure S35. Cyclic voltammogram of **3-CAAC^{Me}**. Formal potentials for oxidation: $E_{1/2} = -1.00\text{V}$ (reversible), $E_{\text{pa}} = 0.03\text{ V}$ (irreversible); for reduction: $E_{\text{pc}} = -2.68$ (irreversible).

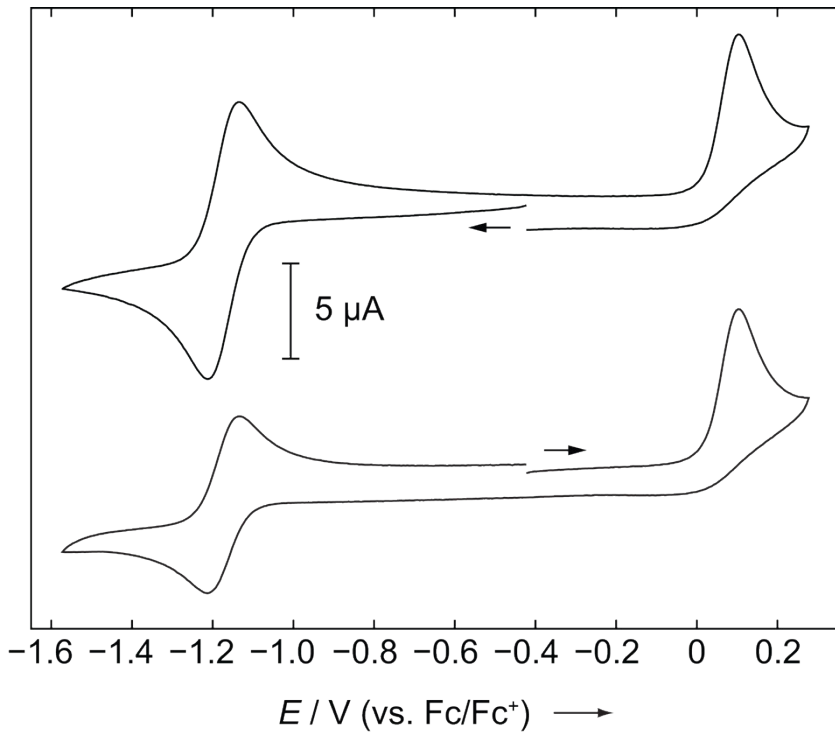


Figure S36. Cyclic voltammograms of **3-IMes** with different scan directions in THF. Formal potentials for oxidation: $E_{1/2} = -1.17\text{ V}$ (reversible) and $E_{\text{pa}} = +0.11\text{ V}$ (irreversible). No reduction wave was observed down to -3.20 V .

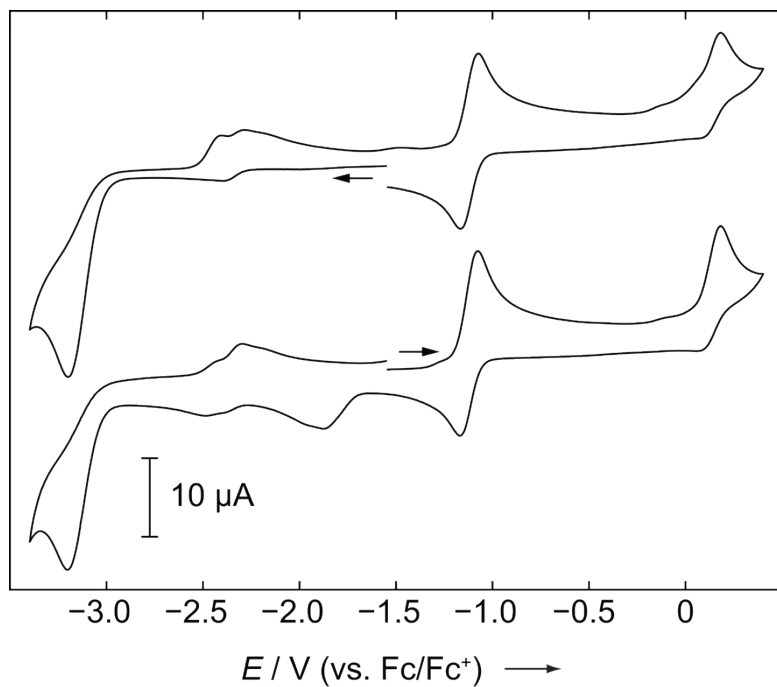


Figure S37. Cyclic voltammograms of **3-SIMes** with different scan directions in THF. Formal potentials for oxidation: $E_{1/2} = -1.11 \text{ V}$, $E_{\text{pa}} = +0.19 \text{ V}$ (broad corresponding reduction waves at ca. -1.8 V and -2.3 V); for reduction: $E_{\text{pc}} = -3.17 \text{ V}$ (irreversible).

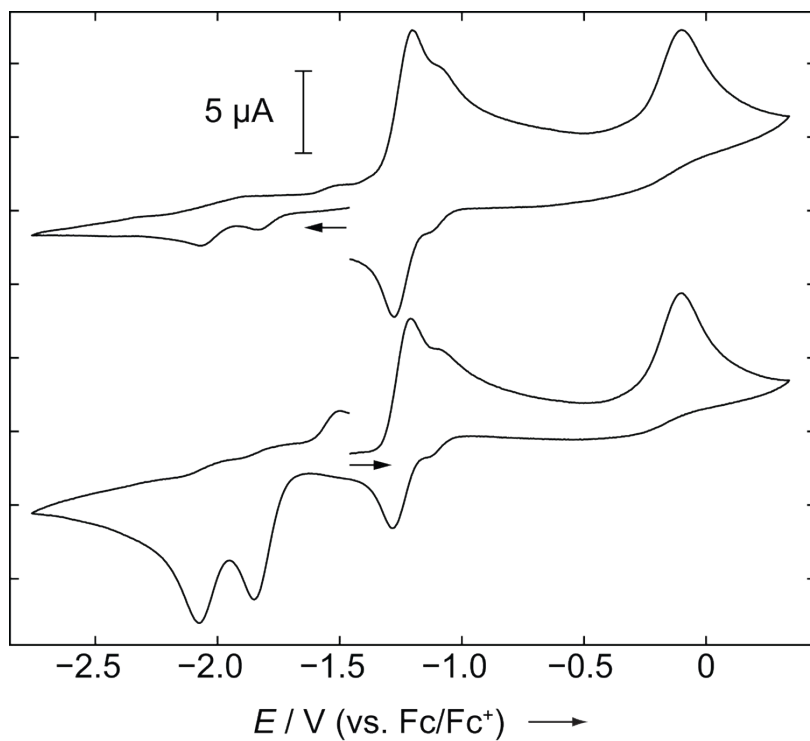


Figure S38. Cyclic voltammograms of **3-IMeMe** with different scan directions in THF. Formal potentials for oxidation: $E_{1/2} = -1.26 \text{ V}$ and $E_{\text{pa}} = -0.11 \text{ V}$ (corresponding reduction waves at -1.80 V and -2.07 V).

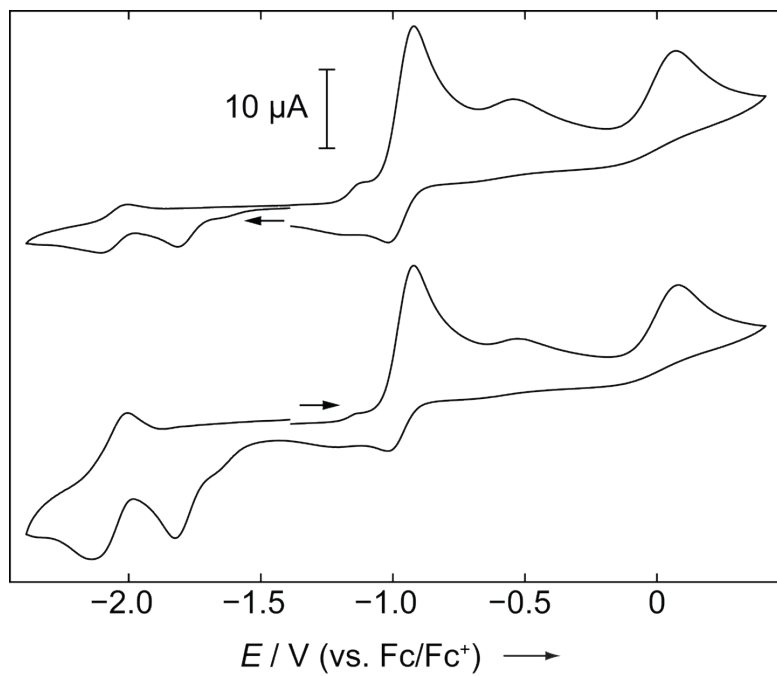


Figure S39. Cyclic voltammograms of **3**-**PEt**₃ with different scan directions in THF. Formal potentials for oxidation: $E_{1/2} = -0.97$ V, $E_{pa} = -0.54$ V, and $E_{pa} = +0.07$ V (corresponding reduction waves at -1.81 V and -2.05 V).

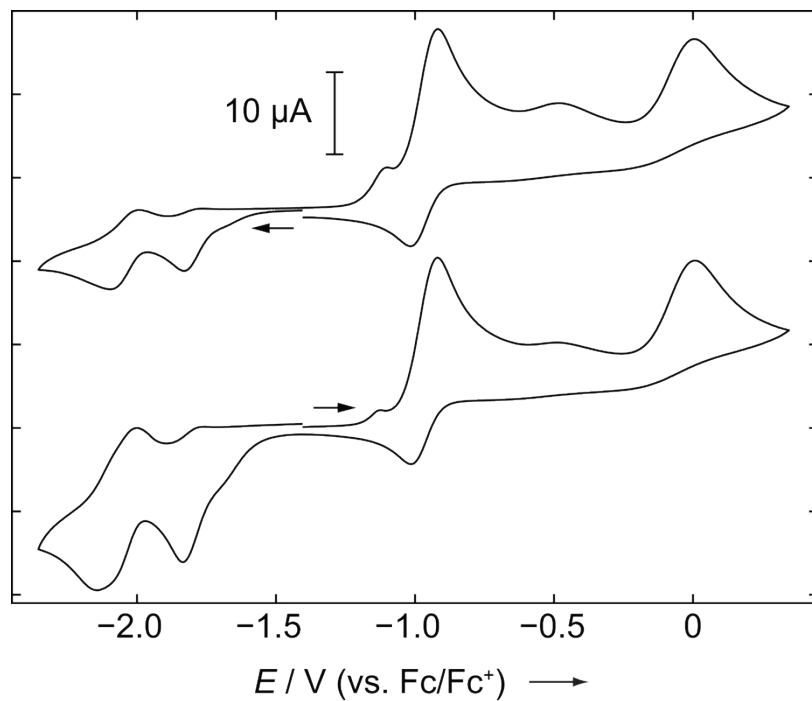


Figure S40. Cyclic voltammograms of **3**-**PMMe**₃ with different scan directions in THF. Formal potentials for oxidation: $E_{1/2} = -0.95$ V, $E_{pa} = -0.49$ V and $E_{pa} = +0.05$ V (corresponding reduction waves at -1.80 V and -2.02 V).

X-ray crystallographic data

Crystal data of all compounds were collected on a Bruker X8-APEX II diffractometer with a CCD area detector (compounds **2**, **3-L**, L = CAAC^{Me}, IMes, IMe^{Me}, PEt₃, PMe₃, **4**, **6** and **7**) or a BRUKER D8 QUEST diffractometer with a CMOS area detector (compounds **1**, **3-SIMes** and **5**), each equipped with *m*-layer mirror monochromated Mo_{Kα} radiation. The structures were solved using intrinsic phasing methods,⁶ refined with the ShelXL software package⁷ and expanded using Fourier techniques. All non-hydrogen atoms were refined anisotropically. Hydrogen atoms were refined isotropically and assigned to idealised positions, except for boron-bound hydrogen atoms, which were located in the difference Fourier map and freely refined. Cif files of crystallographic structures have been deposited with the Cambridge Crystallographic Data Centre, CCDC numbers 1893541 (**2**), 1893542 (**3-CAAC^{Me}**), 1893543 (**3-PEt₃**), 1893544 (**3-IMes**) 1893545 (**3-PMe₃**), 1893546 (**5-CAAC^{Me}**), 1893547 (**3-SIMes**), 1893548 (**3-IMe^{Me}**), 1893549 (**4**), 1893550 (**6**), 1893551 (**7**), 1893552 (**1**).

Refinement details for 4: The asymmetric unit contains half of a highly disordered and partially occupied hexane molecule positioned on an inversion center, which could not be sensibly modelled. The Platon program Squeeze was therefore applied to deal with electron density in the structural voids. Squeeze detected 232 electrons in the voids, which would correspond to a ca. 2.7 hexane molecule per unit cell.

Refinement details for 3-SIMes: The asymmetric unit contains a highly disordered solvent molecule, resulting from the co-crystallisation of both toluene and benzene solvent, adjacent to an inversion center which could not be sensibly modelled. The Platon program Squeeze was therefore applied to deal with electron density in the structural voids. Squeeze detected 88 electrons in the voids, which would correspond to a ca. 0.3:0.7 benzene-to-toluene ratio in the unit cell.

Refinement details for 6: The THF at O2 was modelled as two-fold disordered in a 3:1 ratio. The anisotropic displacement factors of the THF adduct were modelled with SIMU and DELU restraints.

Crystal data for 1. Formula: C₂₀H₃₁BCl₃N, $M_r = 402.62$, colourless plate, 0.289 × 0.159 × 0.092 mm³, monoclinic space group $P\bar{2}_1/n$, $a = 16.2908(6)$ Å, $b = 8.8180(2)$ Å, $c = 16.4186(6)$

\AA , $\beta = 118.7270(10)^\circ$, $V = 2068.28(12)$ \AA^3 , $Z = 4$, $\rho_{calcd} = 1.293 \text{ g}\cdot\text{cm}^{-3}$, $\mu = 0.447 \text{ mm}^{-1}$, $F(000) = 856$, $T = 100(2)$ K, $R_I = 0.0282$, $wR^2(\text{all}) = 0.0676$, 4210 independent reflections [$2\theta \leq 52.742^\circ$] and 234 parameters.

Crystal data for 2. Formula: $\text{C}_{20}\text{H}_{31}\text{BCl}_2\text{N}$, $M_r = 367.17$, orange block, $0.410 \times 0.220 \times 0.160 \text{ mm}^3$, monoclinic space group $P 2_1/n$, $a = 10.8935(9)$ \AA , $b = 9.2955(7)$ \AA , $c = 20.3854(17)$ \AA , $\beta = 98.385(3)^\circ$, $V = 2042.2(3)$ \AA^3 , $Z = 4$, $\rho_{calcd} = 1.194 \text{ g}\cdot\text{cm}^{-3}$, $\mu = 0.320 \text{ mm}^{-1}$, $F(000) = 788$, $T = 103(2)$ K, $R_I = 0.0433$, $wR^2(\text{all}) = 0.1098$, 4507 independent reflections [$2\theta \leq 54.204^\circ$] and 225 parameters.

Crystal data for 3-CAAC^{Me}. Formula: $\text{C}_{47}\text{H}_{70}\text{BClN}_2$, $M_r = 709.31$, purple block, $0.323 \times 0.158 \times 0.138 \text{ mm}^3$, monoclinic space group $C 2/c$, $a = 12.9399(13)$ \AA , $b = 14.8972(14)$ \AA , $c = 21.640(2)$ \AA , $\beta = 98.624(3)^\circ$, $V = 4124.4(7)$ \AA^3 , $Z = 4$, $\rho_{calcd} = 1.142 \text{ g}\cdot\text{cm}^{-3}$, $\mu = 0.127 \text{ mm}^{-1}$, $F(000) = 1552$, $T = 103(2)$ K, $R_I = 0.0440$, $wR^2(\text{all}) = 0.1051$, 4085 independent reflections [$2\theta \leq 52.142^\circ$] and 272 parameters.

Crystal data for 3-IMes. Formula: $\text{C}_{41}\text{H}_{55}\text{BClN}_3$, $M_r = 636.14$, red plate, $0.260 \times 0.080 \times 0.040 \text{ mm}^3$, monoclinic space group $P 2_1$, $a = 12.5496(12)$ \AA , $b = 16.2449(16)$ \AA , $c = 18.6655(18)$ \AA , $\beta = 103.896(3)^\circ$, $V = 3693.9(6)$ \AA^3 , $Z = 4$, $\rho_{calcd} = 1.144 \text{ g}\cdot\text{cm}^{-3}$, $\mu = 0.135 \text{ mm}^{-1}$, $F(000) = 1376$, $T = 103(2)$ K, $R_I = 0.0607$, $wR^2(\text{all}) = 0.1080$, 14317 independent reflections [$2\theta \leq 52.044^\circ$] and 857 parameters.

Crystal data for 3-SIMes. Formula: $\text{C}_{41}\text{H}_{57}\text{BClN}_3$, $M_r = 638.15$, red plate, $0.409 \times 0.236 \times 0.200 \text{ mm}^3$, triclinic space group $P \bar{1}$, $a = 10.8472(10)$ \AA , $b = 11.1775(10)$ \AA , $c = 18.8985(16)$ \AA , $\alpha = 79.591(4)^\circ$, $\beta = 76.738(4)^\circ$, $\gamma = 71.310(4)^\circ$, $V = 2098.3(3)$ \AA^3 , $Z = 2$, $\rho_{calcd} = 1.010 \text{ g}\cdot\text{cm}^{-3}$, $\mu = 0.119 \text{ mm}^{-1}$, $F(000) = 692$, $T = 100(2)$ K, $R_I = 0.0561$, $wR^2(\text{all}) = 0.1566$, 9250 independent reflections [$2\theta \leq 54.202^\circ$] and 429 parameters.

Crystal data for 3-PEt₃. Formula: $\text{C}_{26}\text{H}_{46}\text{BClNP}$, $M_r = 449.87$, yellow block, $0.590 \times 0.213 \times 0.138 \text{ mm}^3$, monoclinic space group $P 2_1/n$, $a = 15.725(2)$ \AA , $b = 10.7595(14)$ \AA , $c = 17.237(3)$ \AA , $\beta = 117.084(6)^\circ$, $V = 2596.5(7)$ \AA^3 , $Z = 2$, $\rho_{calcd} = 1.151 \text{ g}\cdot\text{cm}^{-3}$, $\mu = 0.222 \text{ mm}^{-1}$, $F(000) = 984$, $T = 103(2)$ K, $R_I = 0.0482$, $wR^2(\text{all}) = 0.1253$, 5718 independent reflections [$2\theta \leq 54.204^\circ$] and 282 parameters.

Crystal data for 3-PMe₃. Formula: C₂₃H₄₀BClN₃, $M_r = 407.79$, very pale yellow block, 0.450 × 0.251 × 0.172 mm³, triclinic space group $P\bar{1}$, $a = 9.5037(5)$ Å, $b = 10.6623(5)$ Å, $c = 14.1920(6)$ Å, $\alpha = 109.040(2)^\circ$, $\beta = 92.350(3)^\circ$, $\gamma = 116.165(2)^\circ$, $V = 1190.80(10)$ Å³, $Z = 2$, $\rho_{calcd} = 1.137$ g·cm⁻³, $\mu = 0.236$ mm⁻¹, $F(000) = 444$, $T = 100(2)$ K, $R_I = 0.0417$, $wR^2(\text{all}) = 0.1114$, 5655 independent reflections [$2\theta \leq 55.950^\circ$] and 255 parameters.

Crystal data for 3-IMe^Me. Formula: C₂₇H₄₃BClN₃, $M_r = 455.90$, orange plate, 0.312 × 0.212 × 0.072 mm³, triclinic space group $P\bar{1}$, $a = 9.1055(16)$ Å, $b = 10.5101(19)$ Å, $c = 13.919(3)$ Å, $\alpha = 87.330(4)^\circ$, $\beta = 88.935(4)^\circ$, $\gamma = 77.336(5)^\circ$, $V = 1298.2(4)$ Å³, $Z = 2$, $\rho_{calcd} = 1.166$ g·cm⁻³, $\mu = 0.166$ mm⁻¹, $F(000) = 496$, $T = 100(2)$ K, $R_I = 0.0520$, $wR^2(\text{all}) = 0.1337$, 5759 independent reflections [$2\theta \leq 54.376^\circ$] and 301 parameters.

Crystal data for 4. Formula: C₄₂H₆₈B₂Cl₂K₂N₂S, $M_r = 874.66$, yellow needle, 0.520 × 0.160 × 0.150 mm³, monoclinic space group $C\bar{2}/c$, $a = 22.7921(16)$ Å, $b = 17.8985(11)$ Å, $c = 14.2655(11)$ Å, $\beta = 105.321(2)^\circ$, $V = 5612.7(7)$ Å³, $Z = 4$, $\rho_{calcd} = 1.035$ g·cm⁻³, $\mu = 0.422$ mm⁻¹, $F(000) = 1864$, $T = 103(2)$ K, $R_I = 0.0473$, $wR^2(\text{all}) = 0.1285$, 6701 independent reflections [$2\theta \leq 55.754^\circ$] and 249 parameters.

Crystal data for 5-CAAC^Me. C₄₀H₆₃BN₂·(C₇H₈)_{0.5}, $M_r = 628.80$, orange block, 0.531 × 0.53 × 0.288 mm³, triclinic space group $P\bar{1}$, $a = 9.1887(11)$ Å, $b = 11.6671(16)$ Å, $c = 18.914(3)$ Å, $\alpha = 78.726(5)^\circ$, $\beta = 77.377(4)^\circ$, $\gamma = 88.791(4)^\circ$, $V = 1940.0(4)$ Å³, $Z = 2$, $\rho_{calcd} = 1.076$ g·cm⁻³, $\mu = 0.061$ mm⁻¹, $F(000) = 694$, $T = 100(2)$ K, $R_I = 0.0802$, $wR^2 = 0.1427$, 7920 independent reflections [$2\theta \leq 52.944^\circ$] and 512 parameters.

Crystal data for 6. Formula: C₅₃H₇₉BLiN₃O₃, $M_r = 823.94$, orange needle, 0.281 × 0.124 × 0.090 mm³, monoclinic space group $P\bar{2}_1/c$, $a = 11.7584(9)$ Å, $b = 20.9712(15)$ Å, $c = 19.9511(14)$ Å, $\beta = 90.364(4)^\circ$, $V = 4919.6(6)$ Å³, $Z = 4$, $\rho_{calcd} = 1.122$ g·cm⁻³, $\mu = 0.067$ mm⁻¹, $F(000) = 1800$, $T = 100(2)$ K, $R_I = 0.0710$, $wR^2(\text{all}) = 0.1757$, 10786 independent reflections [$2\theta \leq 54.206^\circ$] and 614 parameters.

Crystal data for 7. Formula: [C₄₁H₅₇BN₃][C₁₂H₃₀LiO₆] (+ squeezed hexane), $M_r = 880.00$, red block, 0.21 × 0.18 × 0.12 mm³, monoclinic space group $P\bar{2}_1/c$, $a = 27.0965(9)$ Å, $b = 11.3646(4)$ Å, $c = 37.7243(13)$ Å, $\beta = 90.738(2)^\circ$, $V = 11615.9(7)$ Å³, $Z = 8$, $\rho_{calcd} = 1.006$

$\text{g}\cdot\text{cm}^{-3}$, $\mu = 0.064 \text{ mm}^{-1}$, $F(000) = 3856$, $T = 100(2) \text{ K}$, $R_I = 0.0692$, $wR^2(\text{all}) = 0.1913$, 23734 independent reflections [$2\theta \leq 54.756^\circ$] and 1296 parameters.

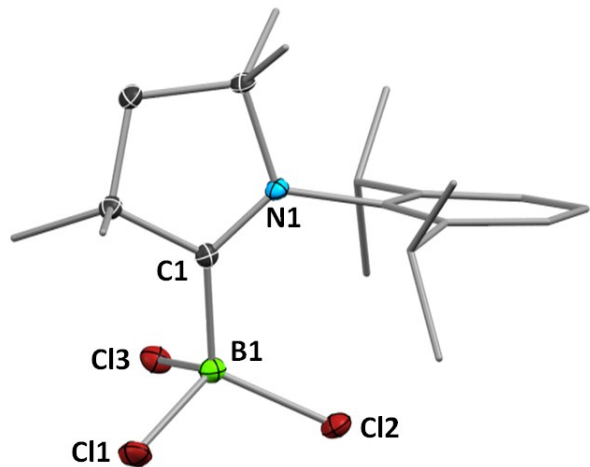


Figure S41. Crystallographically-derived molecular structure of **1**. Thermal ellipsoids drawn at 50% probability level. Ellipsoids on the CAAC^{Me} ligand periphery and hydrogen atoms omitted for clarity. Selected bond lengths (\AA): B1-C1 1.644(2), B1-Cl1 1.8844(17), B1-Cl2 1.8382(17), B1-Cl3 1.8382(17), C1-N1 1.3041(18).

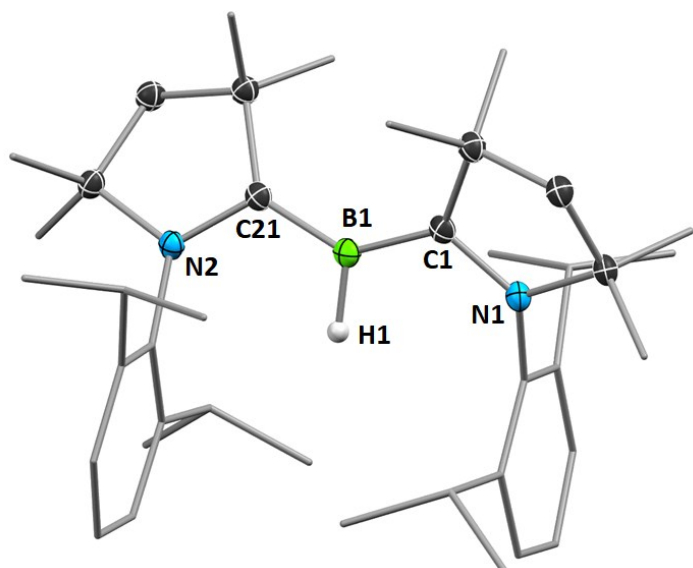


Figure S42. Crystallographically-derived molecular structure of **5**. Thermal ellipsoids drawn at 50% probability level. Ellipsoids on the CAAC^{Me} ligand periphery and hydrogen atoms omitted for clarity. Selected bond lengths (\AA) and angles ($^\circ$): B1-C1 1.510(3), B1-C21 1.508(3), B1-H1 1.104(19), C1-N1 1.383(2), $\Sigma(\angle\text{B1})$ 360.0(12), torsion angle (N1,C1,B1,H1) 16.4(10), torsion angle (N2,C21,B1,H1) 17.4(10).

Computational details

Geometry optimisations and harmonic frequency calculations were performed using the Gaussian09 program package.⁸ Based on a careful evaluation study of Minenkov et al.⁹ geometry optimisations were performed employing the ω B97XD density functional¹⁰ together with the Stuttgart-Dresden effective core potentials¹¹ for all non hydrogen atoms. The corresponding standard valence basis sets ([2s2p] for B and C, [2s3p] for N) were augmented each by a single d-polarisation function.¹² The D95 double- ξ basis¹³ was used for Hydrogen. This basis set combination is abbreviated SDD* in the following. Optimised structures were characterised as minima by eigenvalue analysis of the computed Hessians. Single-point calculations were conducted on the optimised geometries using the M06-2X functional¹⁴ in combination with the 6-311G(d,p) basis set¹⁵ and the ‘ultrafine’ grid option for molecular orbitals and spin densities; also the wave functions used for bonding analysis were obtained at this level of theory. Natural bond orbital (NBO) and natural resonance theory (NRT) calculations were performed using the NBO 6.0 program¹⁶ interfaced with Gaussian09.^{17,18} Pictures of molecular structures were generated with the Cylview¹⁹ and ChemCraft²⁰ programs.

Frontier MOs and spin density of radical 2

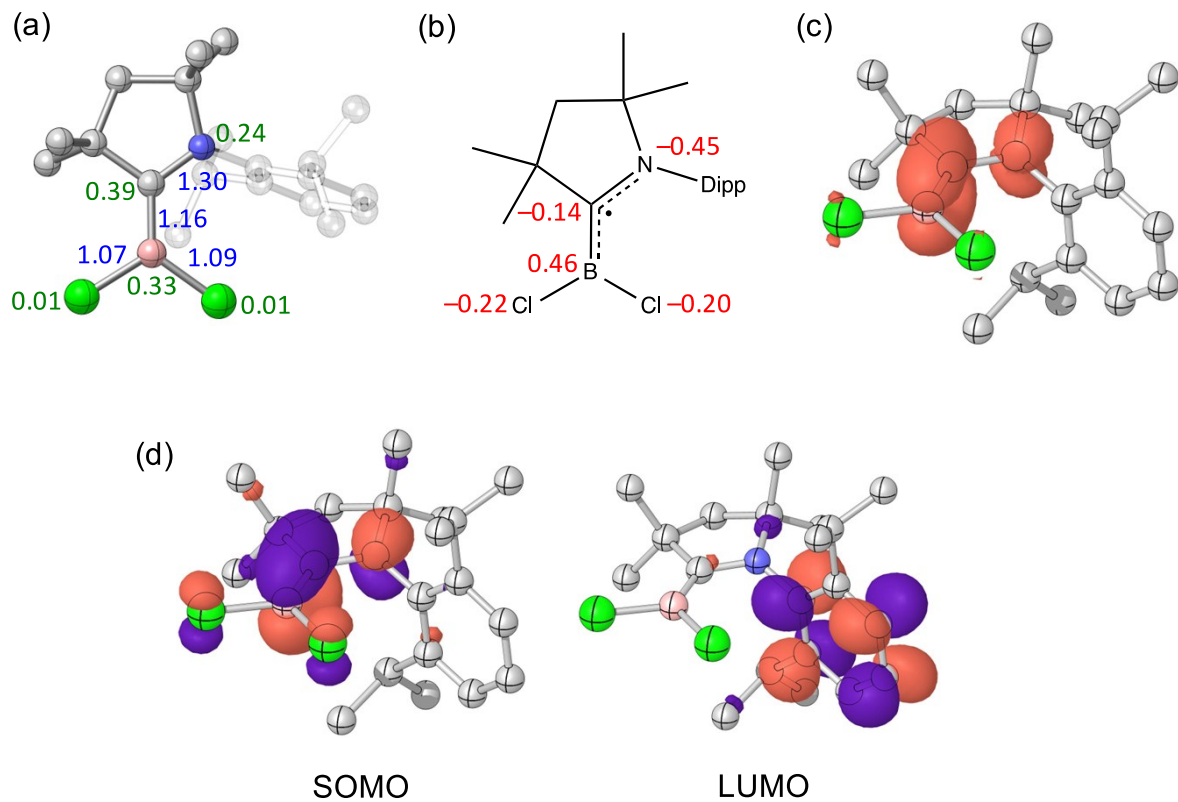


Figure S43. (a) Optimised structure with spin densities in green and Wiberg bond indices in blue. (b) Lewis structure with NPA charges in red. (c) Spin density (isovalue 0.005 a_0^{-3}). (d) Frontier molecular orbitals of **2** (isovalue $\pm 0.05 \text{ a}_0^{-3/2}$).

Frontier MOs and bonding situation in 3-PMe₃

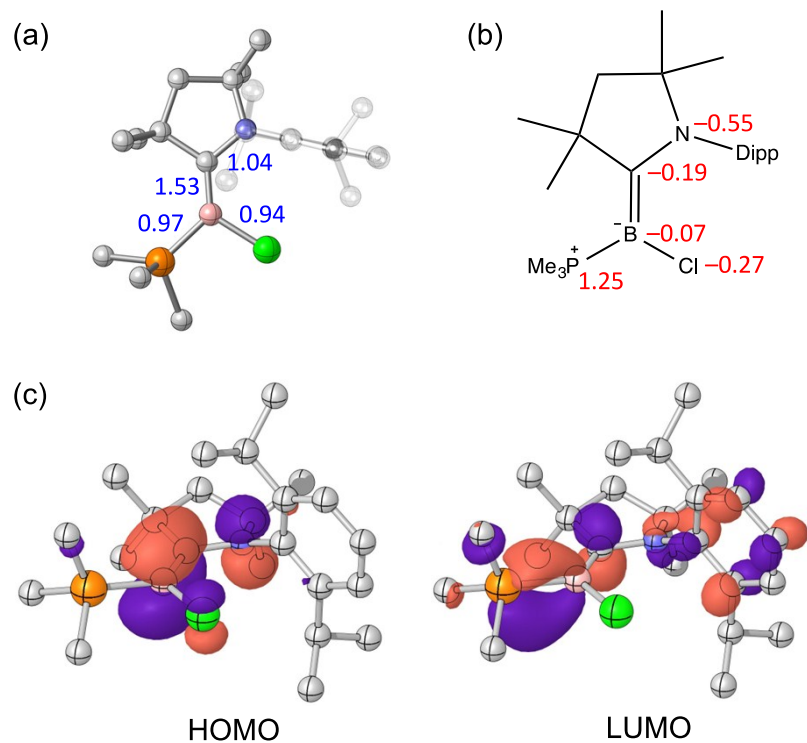


Figure S44. (a) Optimised structure with Wiberg bond indices in blue. (b) Dominant Lewis structure according to NRT analysis with NPA charges in red. (c) Frontier molecular orbitals of 3-PMe₃ (isovalue $\pm 0.05 \text{ } a_0^{-3/2}$).

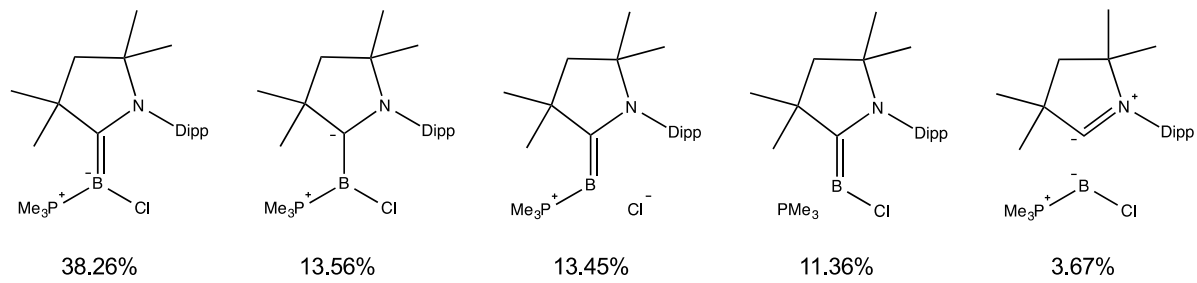


Figure S45. NRT analysis of 3-PMe₃.

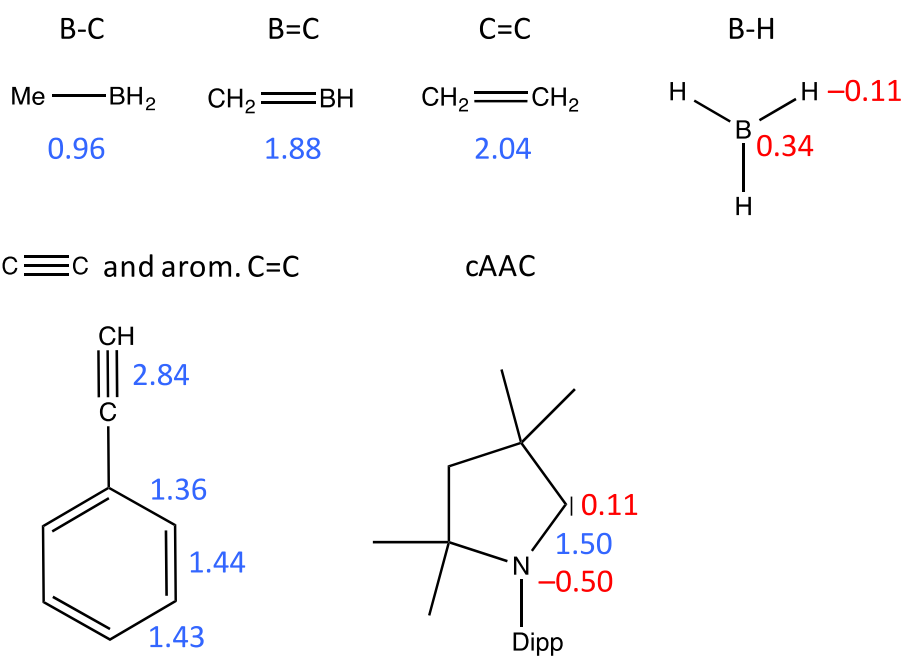


Figure S46. Computed Wiberg bond indices (blue) and NPA charges (red) for selected references systems.

Table S1. Cartesian coordinates of optimised structures

Compound (point group): total energy/Hartree (M06-2X/6-311G(d,p)//wB97XD/SDD*)

2 (C₁): E_{tot} = -1780.72070271				H	2.49648	-3.63232	-1.52290	H	0.24301	1.60478	1.74952	
C				C	3.29381	-2.43079	0.80597	C	1.45200	1.77281	3.49623	
I	-0.04694	-0.16522	-2.70042	H	4.30975	-2.21286	0.45526	H	0.79150	2.53471	3.92769	
C	-1.26153	-0.42959	-0.04206	H	3.21245	-3.51577	0.93959	H	2.30535	2.28103	3.03396	
N	-0.09212	-0.33193	0.66400	H	3.17962	-1.95291	1.78528	H	1.83664	1.16643	4.32454	
B	-1.38903	-0.37665	-1.54414	3-PM₃ (C₁): E_{tot} = -1781.52707287				C	-0.47170	0.17858	3.16554	
C					C					-1.15664	0.88931	3.64698
I	-2.98043	-0.53933	-2.35842	C					H	-0.09383	-0.50356	3.93743
C	-0.24902	-0.68644	2.10853	I	-0.66863	-2.28394	0.11219	H	-1.03342	-0.40993	2.43521	
C	0.62072	0.18364	3.01084	P	-3.29525	-0.91568	-0.14413	C	-3.73889	-2.62705	-0.62619	
H	1.68650	0.02351	2.81838	N	0.73238	0.74516	-0.44273	H	-4.82662	-2.74872	-0.59118	
H	0.41997	-0.07844	4.05526	C	-0.66882	0.60606	-0.48797	H	-3.26581	-3.34200	0.04876	
H	0.40426	1.24734	2.88162	C	1.19979	2.04571	-0.96660	H	-3.37625	-2.81928	-1.64010	
C	0.08945	-2.16232	2.37012	C	2.44234	2.55647	-0.23969	C	-4.53620	0.03514	-1.11129	
H	1.16595	-2.34139	2.33635	H	2.71474	3.54016	-0.63896	H	-5.53149	-0.33720	-0.84553	
H	-0.39076	-2.82499	1.64510	H	3.29449	1.88338	-0.38008	H	-4.36781	-0.13720	-2.17806	
H	-0.26052	-2.44049	3.37047	H	2.26526	2.66041	0.83488	H	-4.49793	1.10698	-0.91560	
C	-1.74350	-0.42240	2.31032	C	1.50672	1.99642	-2.47650	C	-3.90874	-0.80178	1.58466	
H	-1.88170	0.61449	2.63999	H	1.56272	3.01169	-2.88761	H	-4.96034	-1.10032	1.65871	
H	-2.17543	-1.06825	3.08116	H	0.73741	1.44385	-3.02334	H	-3.78720	0.22167	1.95087	
C	-2.42593	-0.61931	0.93920	H	2.46630	1.51093	-2.66994	H	-3.29714	-1.46200	2.20756	
C	-3.51220	0.45964	0.77614	C	-0.01831	2.93257	-0.67979	B	-1.40455	-0.63174	-0.30767	
H	-3.06964	1.46211	0.73885	H	-0.10153	3.77427	-1.37662	BH₃ (D_{3H}): E_{tot} = -26.5920621002				
H	-4.19078	0.41918	1.63784	H	0.08497	3.35652	0.32686	H	0.00000	1.19400	0.00000	
H	-4.10501	0.31584	-0.12827	C	-1.25656	2.01200	-0.73656	B	0.00000	0.00000	0.00000	
C	-3.07701	-2.00772	0.81723	C	-2.22786	2.45243	0.37201	H	-1.03403	-0.59700	0.00000	
H	-3.53696	-2.13860	-0.16565	H	-2.47898	3.51534	0.25716	H	1.03403	-0.59700	0.00000	
H	-3.86097	-2.11765	1.57669	H	-1.77954	2.30983	1.36076	C₂H₄ (D_{2H}): E_{tot} = -78.5622322833				
H	-2.35277	-2.81532	0.95926	H	-3.16933	1.89634	0.35798	C	0.00000	0.00000	0.66789	
C	1.08564	0.32794	0.16827	C	-1.94204	2.14242	-2.10702	H	0.00000	-0.92996	1.22778	
C	1.07051	1.73481	0.08895	H	-2.39818	3.13528	-2.21876	C	0.00000	0.00000	-0.66789	
C	-0.12895	2.57542	0.50205	H	-2.71890	1.38826	-2.24128	H	0.00000	-0.92996	1.22778	
H	-0.82262	1.93307	1.04961	H	-1.22775	2.00763	-2.92300	C	0.00000	0.00000	-0.66789	
C	-0.87985	3.12164	-0.71904	C	1.58660	-0.11560	0.31135	H	0.00000	-0.92996	-1.22778	
H	-0.23281	3.77626	-1.31513	C	2.42824	-1.03519	-0.34100	H	0.00000	-0.92996	-1.22778	
H	-1.75283	3.70445	-0.40113	C	2.43546	-1.19706	-1.84970	H	0.00000	0.92996	-1.22778	
H	-1.22813	2.31648	-1.37229	H	1.65022	-0.54997	-2.24526	cAAC^Me (C₁): E_{tot} = -835.335371927				
C	0.25977	3.72253	1.44457	C	3.78391	-0.76909	-2.44525	C	-1.29811	-0.20962	1.39319	
H	0.85484	3.36739	2.29313	H	3.73742	-0.75307	-3.54096	C	-2.70168	-0.63010	0.93173	
H	-0.64217	4.20648	1.83641	H	4.57665	-1.46953	-2.15442	H	-2.84127	-1.70362	1.10473	
H	0.84419	4.49240	0.92812	H	4.08689	0.22556	-2.09939	H	-3.48315	-0.10855	1.49465	
C	2.20008	2.37877	-0.41223	C	2.09705	-2.62924	-2.28285	C	-2.75606	-0.33016	-0.58871	
H	2.20510	3.46231	-0.49929	H	2.05222	-2.68932	-3.37757	C	-1.31767	-0.16296	-1.04369	
C	3.32145	1.66172	-0.80240	H	1.13059	-2.94032	-1.87767	N	-0.59946	-0.10219	0.05011	
H	4.19413	2.18170	-1.18767	H	2.85637	-3.34460	-1.94333	C	-1.29465	1.13709	2.12293	
C	3.32311	0.27945	-0.70464	C	3.26540	-1.84714	0.42418	H	-1.78090	1.01992	3.09759	
H	4.20275	-0.27590	-1.02094	H	3.92212	-2.55789	-0.07316	H	-1.84072	1.90606	1.56917	
C	2.20852	-0.41357	-0.23298	C	3.25680	-1.78495	1.80863	H	-0.27270	1.49063	2.29833	
C	2.25078	-1.93055	-0.20391	H	3.90470	-2.43493	2.39122	C	-0.64062	-1.25011	2.30030	
H	1.26483	-2.28408	0.10566	C	2.41059	-0.89045	2.44694	H	-1.18234	-1.28752	3.25175	
C	2.52483	-2.53797	-1.58628	H	2.40164	-0.84927	3.53419	H	0.40317	-0.99682	2.51543	
H	3.51467	-2.25379	-1.96287	C	1.57959	-0.03970	1.72003	H	-0.67384	-2.25077	1.86143	
H	1.77874	-2.21562	-2.31665	C	0.68112	0.92158	2.47914					

C	-3.48048	0.99037	-0.89874	C	0.00000	-1.20815	-1.50878
H	-4.53787	0.91872	-0.61540	C	0.00000	1.20815	-1.50878
H	-3.42069	1.21622	-1.96822	H	0.00000	2.15459	0.42386
H	-3.03993	1.83473	-0.35527	H	0.00000	-2.15459	0.42386
C	-3.41592	-1.46841	-1.37200	H	0.00000	-2.14962	-2.05185
H	-2.88231	-2.41385	-1.21606	H	0.00000	2.14962	-2.05185
H	-3.40770	-1.25216	-2.44512	H	0.00000	0.00000	-3.29299
H	-4.45600	-1.60816	-1.05060	C	0.00000	0.00000	2.01853
C	0.82838	0.08381	-0.01011	H	0.00000	0.00000	4.28438
C	3.57861	0.42365	-0.00056	C	0.00000	0.00000	3.21938
C	1.35474	1.38450	-0.05246				
C	1.65616	-1.04890	-0.06454				
C	3.03721	-0.85319	-0.04505				
C	2.74249	1.53052	-0.03151				
H	3.70231	-1.71193	-0.08447				
H	3.17836	2.52557	-0.06295				
H	4.65677	0.55751	0.02185				
C	0.47285	2.60114	-0.27800				
H	-0.55425	2.33147	-0.03214				
C	0.85197	3.80665	0.58607				
H	0.11128	4.60433	0.45869				
H	1.82663	4.22279	0.30604				
H	0.89054	3.54516	1.64966				
C	0.48008	2.95367	-1.77266				
H	-0.18446	3.80396	-1.96914				
H	0.13451	2.09774	-2.36200				
H	1.48948	3.22323	-2.10707				
C	1.09610	-2.44369	-0.28962				
H	0.02652	-2.42299	-0.07311				
C	1.22535	-2.80174	-1.77714				
H	2.27751	-2.82669	-2.08608				
H	0.70078	-2.06031	-2.38918				
H	0.78752	-3.78824	-1.97251				
C	1.73094	-3.50899	0.60776				
H	2.79124	-3.66251	0.37649				
H	1.22630	-4.47118	0.46285				
H	1.65330	-3.23860	1.66682				

H₂CBH (C_S): E_{tot} = -64.6644352180

C	0.00030	-0.59433	0.00000
B	0.00030	0.79000	0.00000
H	-0.92214	-1.17414	0.00000
H	0.91950	-1.17887	0.00000
H	-0.00064	1.96901	0.00000

H₃CBH₂ (C_S): E_{tot} = -65.9152212564

B	-0.01152	0.87735	0.00000
H	1.03573	1.46784	0.00000
H	-1.02419	1.52356	0.00000
C	-0.01152	-0.68615	0.00000
H	0.55594	-1.05028	0.86991
H	0.55594	-1.05028	-0.86991
H	-0.99671	-1.16068	0.00000

PhCCH (C_{2V}): E_{tot} = -308.334012108

C	0.00000	0.00000	0.58769
C	0.00000	0.00000	-2.20593
C	0.00000	1.20882	-0.11234
C	0.00000	-1.20882	-0.11234

References

- 1 R. Jazzar, R. D. Dewhurst, J.-B. Bourg, B. Donnadieu, Y. Canac and G. Bertrand, *Angew. Chem. Int. Ed.*, 2007, **46**, 2899.
- 2 A. J. Arduengo, III, R. Krafczyk, R. Schmutzler, H. A. Craig, J. R. Goerlich, W. J. Marshall and M. Unverzagt, *Tetrahedron*, 1999, **55**, 14523.
- 3 M. S. Viciu, O. Navarro, R. F. Germaneau, R. A. Kelly, III, W. Sommer, N. Marion, E. D. Stevens, L. Cavallo and S. P. Nolan, *Organometallics*, 2004, **23**, 1629.
- 4 N. Kuhn and T. Kratz, *Synthesis*, 1993, **6**, 561.
- 5 D. Savaia, E. Tagliavini, C. Trombini and A. Umani-Ronchi, *J. Org. Chem.*, 1981, **46**, 5344.
- 6 G. Sheldrick, *Acta Cryst.*, 2015, **A71**, 3.
- 7 G. Sheldrick, *Acta Cryst.*, 2008, **A64**, 112.
- 8 M. J. Frisch, G. W. Trucks, H. B. Schlegel, G. E. Scuseria, M. A. Robb, J. R. Cheeseman, G. Scalmani, V. Barone, B. Mennucci, G. A. Petersson, H. Nakatsuji, M. Caricato, X. Li, H. P. Hratchian, A. F. Izmaylov, J. Bloino, G. Zheng, J. L. Sonnenberg, M. Hada, M. Ehara, K. Toyota, R. Fukuda, J. Hasegawa, M. Ishida, T. Nakajima, Y. Honda, O. Kitao, H. Nakai, T. Vreven, J. A. Montgomery, Jr., J. E. Peralta, F. Ogliaro, M. Bearpark, J. J. Heyd, E. Brothers, K. N. Kudin, V. N. Staroverov, R. Kobayashi, J. Normand, K. Raghavachari, A. Rendell, J. C. Burant, S. S. Iyengar, J. Tomasi, M. Cossi, N. Rega, J. M. Millam, M. Klene, J. E. Knox, J. B. Cross, V. Bakken, C. Adamo, J. Jaramillo, R. Gomperts, R. E. Stratmann, O. Yazyev, A. J. Austin, R. Cammi, C. Pomelli, J. W. Ochterski, R. L. Martin, K. Morokuma, V. G. Zakrzewski, G. A. Voth, P. Salvador, J. J. Dannenberg, S. Dapprich, A. D. Daniels, O. Farkas, J. B. Foresman, J. V. Ortiz, J. Cioslowski, D. J. Fox, Gaussian 09, Revision D.01 Gaussian, Inc., Wallingford CT, 2013.
- 9 Y. Minenkov, A. Singstad, G. Occhipinti and V. R. Jensen, *Dalton Trans.*, 2012, **41**, 5526.
- 10 J.-D. Chai and M. Head-Gordon, *Phys. Chem. Chem. Phys.*, 2008, **10**, 6615.
- 11 A. Bergner, M. Dolg, W. Küchle, H. Stoll and H. Preuß, *Mol. Phys.*, 1993, **80**, 1431.
- 12 M. Dupuis, J. D. Watts, H. O. Villar and G. J. B. Hurst, *Comput. Phys. Commun.*, 1989, **52**, 415.
- 13 T. H. Dunning Jr., *J. Chem. Phys.*, 1970, **53**, 2823.
- 14 Y. Zhao and D. Truhlar, *Theor. Chem. Acc.*, 2008, **120**, 215.
- 15 A. D. McLean and G. S. Chandler, *J. Chem. Phys.*, 1980, **72**, 5639.

- 16 E. D. Glendening, J. K. Badenhoop, A. E. Reed, J. E. Carpenter, J. A. Bohmann, C. M. Morales, C. R. Landis and F. Weinhold, NBO 6.0 Theoretical Chemistry Institute, University of Wisconsin, Madison, <http://nbo6.chem.wisc.edu>, 2013.
- 17 E. D. Glendening, C. R. Landis and F. Weinhold, *WIREs Comput. Mol. Sci.*, 2012, **2**, 1.
- 18 E. D. Glendening, C. R. Landis and F. Weinhold, *J. Comput. Chem.*, 2013, **34**, 1429.
- 19 C. Y. Legault, Cylview 1.0b Université de Sherbrooke, <http://www.cylview.org>, 2009.
- 20 G. A. Andrienko, ChemCraft <http://www.chemcraftprog.com>, 2015.